

ISTANBUL TECHNICAL UNIVERSITY ★ GRADUATE SCHOOL OF SCIENCE
ENGINEERING AND TECHNOLOGY

**FERRORESONANCE FAULT DETECTION
IN ELECTRIC POWER NETWORKS
BY ARTIFICIAL NEURAL NETWORKS**



M.Sc. THESIS

Gizem KULAKLI

Faculty of Electrical and Electronics Engineering

Electrical Engineering Programme

AUGUST 2020

ISTANBUL TECHNICAL UNIVERSITY ★ GRADUATE SCHOOL OF SCIENCE
ENGINEERING AND TECHNOLOGY

**FERRORESONANCE FAULT DETECTION
IN ELECTRIC POWER NETWORKS
BY ARTIFICIAL NEURAL NETWORKS**

M.Sc. THESIS

**Gizem KULAKLI
(504171021)**

Department of Electrical Engineering

Electrical Engineering Programme

Thesis Advisor: Assoc. Prof. Dr. Tahir Çetin AKINCI

AUGUST 2020

İSTANBUL TEKNİK ÜNİVERSİTESİ ★ FEN BİLİMLERİ ENSTİTÜSÜ

**ELEKTRİK GÜÇ HATLARINDA
FERROREZONANS ARIZASININ
YAPAY SİNİR AĞLARI İLE BELİRLENMESİ**

YÜKSEK LİSANS TEZİ

**Gizem KULAKLI
(504171021)**

Elektrik Mühendisliği Ana Bilim Dalı

Elektrik Mühendisliği Programı

Tez Danışmanı: Doç. Dr. Tahir Çetin AKINCI

AĞUSTOS 2020

Gizem KULAKLI, a M.Sc student of ITU Graduate School of Science Engineering and Technology student ID 504171021, successfully defended the thesis entitled “FERRORESONANCE FAULT DETECTION IN ELECTRIC POWER NETWORKS BY ARTIFICIAL NEURAL NETWORKS”, which she prepared after fulfilling the requirements specified in the associated legislations, before the jury whose signatures are below.

Thesis Advisor : **Assoc. Prof. Dr. T. Çetin AKINCI**
İstanbul Technical University

Jury Members : **Prof. Dr. Serhat ŞEKER**
İstanbul Technical University

Prof. Dr. Mustafa Caner AKÜNER
Marmara. University

Date of Submission :31 August 2020
Date of Defense :18 September 2020





To my dear family and beloved friends,



FOREWORD

In the thesis process, I would like to thank my esteemed advisor Assoc. Prof. Dr. T. Cetin Akinci who always answers my questions allocates valuable time to me, and does not withhold his motivation and support. It is a great chance for me to work with an advisor like him. I thank him wholeheartedly for his support in the all master process.

I would like to extend my thanks to Karla Frowein who research Assistant Ms Dipl.-Ing working at Dresden Technical University, who guided me for academics during my Erasmus period.

I would like to thanks to Prof. Dr.-Ing. Peter Schegner who accept me during my thesis period at Dresden Technical University.

Thank you (chronologically) to for my father, mother, brother, for supporting me throughout my life, accepting me as who I am and giving me a place where I can always come back.

I would like to thank my dear friends Behnaz Alafi, Büsra Akinci, Koray Yokus, Gül Demirdag, Selma Akyildiz, Uğur Merdamert, Didem Tuzun, Seyma Oksuz, Meltem Sahin who supported me during the postgraduate and thesis writing process.

August 2020

Gizem KULAKLI
(Electrical and Electronics Engineer)



TABLE OF CONTENTS

	<u>Page</u>
FOREWORD.....	ix
TABLE OF CONTENTS.....	xi
ABBREVIATIONS	xiii
SYMBOLS	xv
LIST OF TABLES	xvii
LIST OF FIGURES	xix
SUMMARY	xxi
ÖZET.....	xxii
1. INTRODUCTION.....	1
1.1 Literature Study.....	2
1.2 Outline of the Thesis	3
2. FERRORESONANCE PHENOMENA	5
2.1 Resonance.....	5
2.2 Physical Approach to Ferroresonance.....	6
2.3 Nonlinear Magnetization Characteristic.....	6
2.4 Harmonics	8
2.5 Subharmonics	9
2.6 Type of Ferroresonance.....	10
2.6.1 Soft excitation	10
2.6.2 Hard excitation.....	10
2.7 Ferroresonance Waveforms.....	10
2.7.1 Fundamental mode	10
2.7.2 Subharmonic Mode	11
2.7.3 Quasi-Periodic Mode	11
2.7.4 Chaotic Mode.....	12
2.8 Single Phase Ferroresonance Oscillation	12
2.9 Ferroresonance on Tree Phase System.....	13
3. ARTIFICIAL NEURAL NETWORK	15
3.1 Biological Neuron	15
3.2 Modelling Neuron	16
3.2.1 Single layer	16
3.2.2 Activation function	17
3.2.4 Multiple Layer.....	22
3.3 Artificial Neural Network Models	23
3.3.1 Feed Forward Neural Networks	23
3.3.2 Feedback Neural Networks	24
3.4 Learning Rules in Artificial Neural Networks	24
3.4.1 Error Correction Learning.....	24
3.4.2 Self (Unsupervised) Learning	25
3.4.3 Supervised Learning	25
3.4.4 Reinforcement Learning	25
3.5 According to the learning time	25

3.5.1 Static.....	25
3.5.2 Dynamic	25
3.6 Artificial Neural Network Advantages and Disadvantages.....	26
4. DATA ACQUISITION AND MODELLING	27
4.1 Ferroresonance Detection.....	28
4.1.1 R1 Data.....	28
4.1.2 R2 Data.....	30
4.1.3 R3 Data.....	31
4.1.4 R4 Data.....	32
5. APPLICATION OF ARTIFICIAL NEURAL NETWORK FOR FERRORESONANCE IDENTIFICATION.....	33
5.1 Matlab Tool	33
5.1.1 Variables.....	33
5.2.Results of Training	37
5.2.1 First group of training	37
5.2.2 Second Group of Training.....	42
5.2.3 Third Group of Training.....	47
5.2.4 Fourth Group of Training.....	51
5.2.5 Fifth Group of Training.....	51
6. CONCLUSION.....	55
REFERENCES	61
APPENDICES	67
APPENDIX A:	67
CURRICULUM VITAE	79

ABBREVIATIONS

ANN	: Artificial Neural Network
BFG	: BFGS Quasi-Newton
CGB	: Conjugate Gradient with Powell/Beale Restarts
CGF	: Fletcher-Powell Conjugate Gradient
CGP	: Polak-Ribiere Conjugate Gradient
CRGO	: Cold Rolled Grain Oriented
GDX	: Variable Learning Rate Backpropagation
LM	: Levenberg-Marquardt
MSE	: Mean Square Error
MSEREG	: Mean squared error w/reg
NARX	: Nonlinear autoregressive exogenous model
MSE	: Mean squared error
MSEREG	: Mean squared error w/reg
OSS.	: One Step Secant
RP	: Resilient Backpropagation
SCG	: Scaled Conjugate Gradient
SSE	: Sum Square Error



SYMBOLS

f	: Resonance frequency
L	: Inductance
C	: Capacitance
\vec{B}	: Magnetic flux density
A	: Area
\vec{H}	: Magnetic field intensity
μ	: Magnetic permeability
ω	: Angular velocity
I_m	: Maximum point of current
I	: Current
t	: Time
C_e	: Ground capacitance of facility
C_g	: Capacitance of circuit breaker
w	: Angular velocity
V	: Voltage source
v	: Neuron's response partner addition
R_{Fe}	: Inductive reactance
L_H	: Non linear main inductance of transformer coil
b	: Bias
α	: Constant gradient
φ	: Activation function
X_i	: Input value
W_i	: Weight value
Y	: Output Value



LIST OF TABLES

	<u>Page</u>
Table 4.1: Parameters of Electrical Components used in Seyitomer-Isiklar Power Networkfor Figure 4.1.....	27
Table 4.2 : Parameters of Electrical Components used in Oymapinar Power Networkfor Figure 4.2.....	28
Table 5.1: Training function table (Demuth & Beale, 2004).	35
Table 5.2 : First Group of Training.	41
Table 5.3 : Second Group of Training.	46
Table 5.4 : Third group of training.....	50
Table 5.5 : Fourth group of training.....	52
Table 5.6 : Fifth group of training.....	53



LIST OF FIGURES

	<u>Page</u>
Figure 2.1 : (a) Parallel resonance circuit (b) Series resonance circuit.....	6
Figure 2.2 : Hysterisis curve (Patsios, et. al 2011).	8
Figure 2.3 : Harmonics plot of the main signal, third and fifth signal and signals with harmonics.	9
Figure 2.4 : Fundamentals mode graphs (Ferracci, 1998).....	11
Figure 2.5 : Subharmonic Mode Graphs (Ferracci, 1998).	11
Figure 2.6 : Quasi-periodic mode graphs (Ferracci, 1998).	12
Figure 2.7 : Chaotic mode graphs (Ferracci, 1998).	12
Figure 2.8 : Single-phase ferroresonance sample circuit.	13
Figure 2.9 : Possible three phase ferroresonant circuit (Csanyi, 2020).	14
Figure 3.1 : Biological neuron (Watson, et al., 2010).....	15
Figure 3.2 : Single layer artificial neural network (Sergio, et al., 2015).	17
Figure 3.3 : Linear function.	18
Figure 3.4 : Logsig function.....	18
Figure 3.5 : Hyperbolic tangent (Tansig) function.	19
Figure 3.6 : Soft-sign function.	20
Figure 3.7 : ReLU function.	20
Figure 3.8 : Soft-plus function.	21
Figure 3.9 : ELU function.	21
Figure 3.10 : Step function.....	22
Figure 3.11: Multiple layers of artificial neural network.....	23
Figure 3.12 : Feed forward neural networks.	24
Figure 3.13 : Feed-back neural networks.....	243
Figure 4. 1: Schematic representation of the transmission line.	27
Figure 4. 2 : Schematic representation of the Oymapinar transmission line.	28
Figure 4. 3: R1 data's plot.....	29
Figure 4.4 : The moment when ferroresonance failure started in R1.	29
Figure 4.5 : R2 data.	30
Figure 4.6 : The moment when ferroresonance failure started in R2.	30
Figure 4.7 : R3 data.....	31
Figure 4.8 : The moment when ferroresonance failure started in R3.	31
Figure 4.9 : R4 data.....	32
Figure 4.10 : The moment when ferroresonance failure started in R4	32
Figure 5.1 : Variables input interface.	34
Figure 5.2 : Performance plot for NN28.....	38
Figure 5.3 : Regression plot for NN28.....	38
Figure 5.4 : Performance plot for NN11.....	39
Figure 5.5 : Regression plot for NN11.....	39
Figure 5.6 : Performance plot for NN12.....	40
Figure 5.7 : Regression plot for NN12.....	40
Figure 5.8 : Performance plot for NN18.....	42
Figure 5.9 : Regression plot for NN18.....	43

Figure 5.10 : Performance plot for NN24.	43
Figure 5.11 : Regression plot for NN24.	44
Figure 5.12 : Performance Plot for NN6.	45
Figure 5.13 : Regression plot for NN6.	45
Figure 5.14 : Performance plot for NN29.	47
Figure 5.15 : Regression plot for NN29.	48
Figure 5.16 : Performance plot for NN30.	48
Figure 5.17 : Regression plot for NN30.	49
Figure 6.1 : First group of training graph.	55
Figure 6.2 : Second group of training graph.	56
Figure 6.3 : Third group of training graph.	56
Figure 6.4 : Chart comparing the first three groups.	57
Figure 6.5 : Fourth group of training graph.	58
Figure 6.6 : Fifth group of training graph.	58
Figure 6.7 : Graph comparing the first and fifth learning groups.	59
Figure A.1 : Performance plot for NN7.	67
Figure A.2 : Performance plot for NN23.	68
Figure A.3 : Regression plot for NN23.	68
Figure A.4 : Performance plot for NN8.	69
Figure A.5 : Regression plot for NN8.	69
Figure A.6 : Performance plot for NN31.	70
Figure A.7 : Regression plot for NN31.	70
Figure A.8 : Performance plot for NN4.	71
Figure A.9 : Performance plot for NN22.	71
Figure A.10 : Regression plot for NN22.	72
Figure A.11 : Performance plot for NN5.	72
Figure A.12 : Regression plot for NN5.	73
Figure A.13 : Performance plot for NN17.	73
Figure A.14 : Regression plot for NN17.	74
Figure A.15 : Performance plot for NN20.	74
Figure A.16 : Performance plot for NN21.	75
Figure A.17 : Regression plot for NN21.	75
Figure A.18 : Performance plot for NN25.	76
Figure A.19 : Regression plot for NN25.	76
Figure A.20 : Performance plot for NN26.	77
Figure A.21 : Regression plot for NN26.	77
Figure A.22 : Performance plot for NN27.	78
Figure A.23 : Regression plot for NN27.	78

FERROREZONANCE FAULT DETECTION IN ELECTRIC POWER NETWORKS BY NEURAL NETWORKS

SUMMARY

Ferroresonance is a complicated nonlinear waving which can appear in electrical circuits with a series or parallel connection of nonlinear inductance and capacitance. Cause of the current of ferroresonance on the transmission line elements such as cables or transformers can be partially or completely damaged. This destruction not only creates huge material losses on the system but also creates unjust suffering.

It is important for the sustainability of the system that a devastating error such as ferroresonance can be detected. If ferroresonance can detecting in advance prevent the loss of time and money for the user by destroying the elements such as power transformer and cables used in the system

Ferroresonance is nonlinear situation and learning in artificial neural networks has advantages such as working with missing or uncertain data, processing real conditions, handling nonlinear situations, being more successful than traditional methods, fault tolerance.

Artificial neural networks are referred to by this name because they are based on learning of the human neural cell in principle. One nerve cell receives information from other cells from the dendrites department, which corresponds to input in artificial neural networks, while axon in human nerve cells corresponds to output in artificial neural networks. Artificial neural networks mainly consist of three layers. There are hidden tabs determined by the number of layers between the input and the output. The learning process is multiplied by the randomly assigned weight value of the input value, and the NET value is created, and if it is determined, the bias others are summed and output from the cell where this total value is found according to the activation function. This output value is the input of the next hidden layer and continues until the same process reaches the output value. The output value gives the result of the learning operation according to the specified value ranges. The activation function is important in solving the problem used. Various activation functions are mentioned in the thesis. A successful algorithm was investigated by using an artificial neural network method to detect ferroresonance error.

In this study, four different ferroresonance data emerging with different scenarios in the transmission line which used energy transmission line modeling from western Anatolia Turkey Seydischir-Oymapınar transmission line has 380 kV were used as input values.

Work steps; literature search on the subject, detection of the moment when ferroresonance starts in voltage outputs, creating input, training and example data from ferroresonance data, to create the appropriate algorithm for nonlinear ferroresonance.

ELEKTRİK GÜÇ HATLARINDA FERROREZONANS ARIZASININ YAPAY SİNİR AĞLARI İLE BELİRLENMESİ

ÖZET

Günümüzde artan enerji ihtiyacı sonucunda iletimde enerji kayıplarının azaltılması için iletim hatlarında gerilim değerleri arttırılma yoluna gidilmiştir, artan gerilimin akımı düşürmesiyle iletim kayıplarının azalması hedeflenmiştir. Aynı zamanda artan enerji ihtiyacı dağıtım ağına da kablo artışına sebep olmaktadır. Oluşan yüksek gerilimler ve artan kablolar hatlardaki kapasitif yükleri arttırmaktadır. Kapasitif yükün artması iletim ve dağıtım hatlarında endüktif transformatör, şönt reaktör, güç trafoları gibi doyuma gidebilen ve lineer olmayan endüktif özellik sergileyebilen manyetik çekirdeğe sahip elektrik makinaların çekirdek endüktanslarının doyuma gitmesine neden olmakta ve doğrusal olmayan endüktans karakteristiğine sebep olmaktadır. Bu doğrusal olmayan karakteristik kararlı ve geçici rejimlerde tahmini zor ani elektriksel hareketlere sebep olmaktadır. Bu tür ani elektriksel olayların yaşanmaması için transformatörler tasarlanırken, sisteme alma sırasında oluşabilecek ani akımları göz önünde bulundurup çekirdek tasarım değerleri, genellikle devreye alma sırasında çekirdekte kullanılan tanecikleri yönlendirilmiş soğuk haddelenmiş silisyumlu demir nüveye ait üretici tarafından verilen akı yoğunluğu ile manyetik alan yoğunluğu grafiğindeki dirsek bölgesi kırılma noktası değerinin kullanılan sacın 0.9 ile 0.85 katı arasında çalışılarak önlem almaktadırlar.

Devredeki öğelerden birinde meydana gelen bu ani değişimler hat üzerindeki elemanların gerilim ve akımlarında ani ve riskli yükselmelere sebep olur. Ferrerezonans, doğrusal olmayan endüktans ve kapasitansın seri veya paralel bağlantısı olan elektrik devrelerinde meydana gelebilecek karmaşık doğrusal olmayan salınımlardır. Pratik tecrübe ve teorik çalışmalara göre bu fenomen, yüksek seviyede harmonik bozulma ile yüksek aşırı gerilim ve aşırı akım oluşumuna yol açar ve geleneksel aşırı gerilim ve aşırı akım baskılama yöntemleriyle ortadan kaldırılamaz. Elektrik şebekelerinde, oluşabilecek ani bir ferrerezonans sonucu ortaya çıkan yüksek akımla sistem üzerindeki koruma ya da iletim elemanlarında maddi olarak kısmi hasarlar ya da geri dönüşü mümkün olmayan kalıcı hasarlar meydana getirebilmektedir. Örneğin kablolarda koruyucu kılıfların erimesi ya da kopması, trafolarda ferrerezonansın olduğu fazda bobinde deformasyonlar, ani akım artışıyla anı ısınma, kazanlarda patlama yırtılma, transformatörlerde yangın, yağ sızması gibi sadece şebekeyi değil çevreyi de etkileyen tehlikeye atan tehlikeli arızaları mümkün kılmakta arızanın meydana geldiği şebekede uzun süreli güç kaynağı kesintisine neden olabilmekte ve bu hat üzerindeki dağıtım ya da iletim şirketinde maddi za zamansal kayıplara sebep olduğu gibi kullanıcılarında enerjisiz kalmasına ve maduriyet yaşamalarına sebep olabilmektedir. Bu nedenle, ferrerezonans arızasından kesinlikle kaçınılması gerekir. Ağın işleyişinde ferrerezonansın neden olduğu arızaların sayısı azaltılmadığından, verilen sorun günümüzde önemlidir.

Elektriksel güç sistemlerinde, ferreazonans, temel frekansta veya subharmonik veya daha yüksek dereceli harmonik frekanslardan birinde oluşabilir. Doğrusal olmayan transformatör bu akım ve gerilim harmoniklerini tanıtır. Ferreazonans, bir kapasitans ve bir endüktans bu harmoniklerden birine girdiğinde ortaya çıkar. Ferreazonans, temel frekansta meydana gelirken, bazen subharmonik ferreazonans da olabilir. İkinci durumda, ferreazonant aşırı gerilimler daha az şiddetlidir ve hafifletilmesi daha zordur. Bu tür ferreazonans, bazen bir gerilim trafosunun enerjilendirilmiş bir hat boyunca uzanan enerjisiz bir iletim hattına bağlandığı ekstra yüksek gerilim iletim ağında meydana gelir.

Bu çalışmada; Tahir Çetin Akıncı tarafından oluşturulan Türkiye Batı Anadolu enerji iletim hattı parçası olan 380kV'luk Seydişehir-Oymapınar iletim hattı modeli ile model üzerinde muhtemel ferreazonans senaryoları oluşturulmuş R fazına ait dört farklı ferreazonans verisi kullanılmıştır.

Yapay sinir ağları, makine öğreniminin alt dallarından biridir. Günümüzde tıpta hastalık tespiti ya da tahmini, mühendislikte arızaların belirlenmesi, üretim, hata öngörüsü, sosyal ağlarda kişiye özel reklamların gelmesi için kullanıcının ilgi alanlarının tanımlanması gibi pek çok alanda farklı amaçlarla kullanılmaktadır.

Yapay sinir ağları prensipte insan sinir hücresinin öğrenmesini baz aldığı için bu isimle anılmaktadır. Bir sinir hücresi dentrit bölümünden diğer hücrelerden gelen bilgiyi alır bu durum yapay sinir ağlarında inputa tekabül ederken, insan sinir hücresinde akson yapay sinir ağlarında outputa tekabül etmektedir. Yapay sinir ağları temelde üç katmandan oluşur. Input ile output arasında katmansayısı kullanıcı tarafından belirlenen gizli sekmeler bulunmaktadır.

Öğrenme işlemi input değerinin rastgele atanan ağırlık değeri ile çarpılarak NET değerin oluşturulması ve belirlenmişse bias değerlerinin toplanıp bu toplam değerinin aktivasyon fonksiyonuna göre bulunduğu hücreden çıkışı alınır. Bu çıkış değeri bir sonraki gizli katmanın girişi olup aynı işlem çıkış değerine ulaşınca kadar devam eder. Belirlenen değer aralıklarına göre çıkış değeri öğrenme işleminin sonucunu verir. Aktivasyon fonksiyonu kullanılan problemin çözümünde önem teşkil etmektedir. Tezin içerisinde çeşitli aktivasyon fonksiyonlarından bahsedilmiştir.

Ferreazonans gibi yıkıcı etkisi yüksek bu arızanın tespitinde algılamaya göre sınıflandırma veyahut tanıma yapabilmeleri, yapay sinir ağlarının öğrenebilmesi, eksik ya da belirsiz datalarla da çalışabilmesi, gerçek zamanlı bilgiyi işleyebilmesi, lineer olmayan durumları işleyebilmesi, geleneksel yöntemlere göre daha başarılı olması, hata toleransının olması, ferreazonans gibi lineer olmayan ani ortaya çıkan yıkıcı etkisi fazla olan olayın tespitinde avantajlı olacağı için bu durumun tespitinde yapay sinir ağları yönteminin kullanılmasının avantajlı olacağı düşünülmüş ve başarılı bir algoritma araştırılmıştır.

Bu tezde girdi olarak kullandığımız Seydişehir-Oymapınar iletim hattı pi modeli ile modellenmiş olup iletim hattı modeli üzerinde muhtemel ferreazonans senaryoları oluşturulmuş R fazına ait dört farklı ferreazonans datası birleştirilerek input datası öğrenme için kullanılan data oluşturulmuş, Matlab© nntool kullanılarak bu hat üzerinde ki olasılı ferreazonans durumunda hangi algoritmanın, bu algoritmada kullanılan aktivasyon fonksiyonu gibi değerler değiştirilip hangisinin daha optimum olduğu araştırılmıştır.

Tezin hazırlanma aşamasında; literatür çalışması yapılmıştır .Bu safhada konu ile ilgili akademik yayınlar ya da kitaplar araştırılmıştır.

Dört farklı ferreazonans verileri 500 veriden oluşan parçlara ayrılıp, ferreazonans olayının başladığı nokta tespit edilip, ferreazonans olayının meydana geldiği kısımlar her dört veri için toplanıp bu oluşan verilerden giriş değerleri oluşturulmuştur.

Matlab© programı kullanılarak çeşitli algoritmalarla lineer olmayan ferreazonans olayını belirleyen durum için uygun lagoritma arayışına gidilmiştir.





1. INTRODUCTION

Today, as a result of technological advances, the need for energy is increasing. The consumption and need of electricity is increasing every year due to reasons such as preferring electric vehicles instead of petroleum-based fuels, increasing the number of domestic appliance used in the home, producing a special electrical device for every need and an increase in industrialization. Providing quality and reliable electricity that consumers will need in the electrical energy system is of great importance socially and economically. The generation, transmission and distribution of electrical energy is a rather complicated event. During this event, it may be necessary to add new elements to the system or maneuver the system. These events can cause various failures such as ferroresonance (Akinci, et al., 2009), (Dimitriyev, et al., 2003).

Increasing energy demand not only caused a rise in energy production but also increased the elements required for the transmission of energy, for instance underground transmission and distribution cables, circuit protection elements, transformers, capacitors, etc. Energy is transmitted with high voltage in order to minimize losses while transmitting energy. In order to reduce losses that occur in cables, energy is transmitted to high stress. High voltages and increased cables resulting from this increasing energy need increase the capacitive loads in the lines, increase in capacitive load induction transformer, shunt reactor, power transformers, electrical machines with magnetic cores lead to saturation of core inductances and cause non-linear inductance characteristics. This non-linear characteristic of stable and transient regimens difficult to predict sudden electrical movements. Paul Boucherot first used definition of ferroresonance for this nonlinear condition in the 1920s. (Boucherot, 1920) The first analytical experiment and work about ferroresonance were carried out in the 1950s by R. Rudenberg (Rudenberg, 1950) and later in the 1950s by C. Hayashi (Hayashi, 1964).

1.1 Literature Study

There are different approaches to detecting ferroresonance;

Akinci, et al.(2009), investigated the effect of the ferroresonance event, which has a destructive effect on energy transmission lines, in a phase system. In this study, a general approach is obtained by modeling the Ferroresonance event with the ATP package program in the 36 kV transmission systems. FFT analysis of the harmonics formed in the modeled system was made and this analyze and results were evaluated. With the formation of ferroresonance in the transmission line, high-frequency components appeared. High-frequency components dominate between 0 and 2000 Hz by FFT analysis. It can be seen that it contains the working frequency in particular. Although the arrow above 2000 Hz has high amplitude frequencies, it is rarely seen. These frequencies are likely to be inter-harmonics. With the formation of ferroresonance, the system contains high-frequency components other than 50 Hz frequency. These voltage and high-frequency changes are harmful to the system.

Seker, et al. (2011), by using Seyitömer-Işıklar model data to determine the frequency and statistical properties of the event using the voltage values in the R phase, power spectral density approach, and Fourier analysis. In this study, it is mentioned that inter harmonics are important in ferroresonance detection. In this study, frequency-domain analysis and related to the statistical studies were conducted, frequency ranges resulting from ferroresonance are determined and it is concluded that the ferroresonance effect will be explained by inter harmonics.

Sharbain, et al., 2017, In the 60 Hz frequency system, they modeled the 32 km transmission line with the pi section. In this study, it was observed that the highest recognition rate was achieved in Dd6 and after learning the changes in the number of neurons and layers. It has been observed that in most of the tested cases, ferroresonance can be detected with an average accuracy of more than 95%.

Wahyudi, et al.(2017), in this article, maneuvers were performed with cutters in a step-down transformer in 20kV distribution network and ferroresonance was created, this data was used for ANN and it was concluded that ANN is a successful ferroresonance analysis method.

Valverde, et al.(2012), The voltage output in the fundamental ferroresonance mode of the fault generated by the voltage transformer used, Matlab© analysed using artificial

neural network tool and concluded that artificial neural network is extremely successful in determining this malfunction.

1.2 Outline of the Thesis

In this thesis; Western Anatolia, Turkey was part of the power transmission line Seydisehir-Oymapınar transmission fault data obtained models made in accordance with the actual data of the line is used. Four different ferroresonance faults were created with different scenarios from the model and the voltage outputs of this fault were used as the inputs of the neural network used, to use these inputs in the artificial neural network to investigate which algorithm is most suitable for this type of non-linear situation and to be a guide in matters compatible with a neural network that can be developed for this type of failure.

This thesis consists of six main chapters. In the first part, the introduction of the thesis is mentioned. Studies on the subject of the literature survey and ferroresonance are mentioned. In the second part, the phenomenon of ferroresonance is explained. In the third chapter, the artificial neural network is explained, in the fourth chapter; the fractions obtained from the actual modelling of the Seyitömer-Işıklar line and in which scenarios are explained. In the fifth section, various algorithms were created using the Matlab© tool and in the last section, the algorithms tested were compared and the successes of the established algorithms were evaluated.



2. FERRORESONANCE PHENOMENA

Excessive voltages and currents that occur in systems where ferroresonance occurs, especially over-currents, cause the insulation materials to go above their thermal resistance due to the high heat they generate and thus loss of insulation. As a result of this loss of insulation, short circuits occur in the system and irreversible failures may occur (Akgun, et al., 2019). Because in the case of ferroresonant, the voltage in the system can be approximately (1.5-3.5) times the nominal voltage. The fact that these malfunctions are highly charged and cause disruptions in energy transmission and distribution creates both a substantial material record and victimization. Ferroresonance not only causes problems in insulation materials but also causes the protection devices to work and break down untimely. Before understanding ferroresonance, the concept of resonance should be considered. (Pejic, et al., 2017), (Akinci, et al., 2013), (Akinci & Ekren, 2011).

2.1 Resonance

Resonance circuits, capacitive elements and inductor elements are needed for resonance to occur. The resonance circuits are obtained by connecting the inductance in series or parallel a capacitor as shown in figure 2.1. In equation 2.1 and equation 2.2 shows that resonance formula, in formula f is resonance frequency in hertz, L is the inductance in henry, C is the capacitance in farads. For resonance inductive reactance and capacitive reactance must be equal, this equation shows equation 2.3.

$$\omega = 2\pi f \quad (2.1)$$

$$\omega L = \frac{1}{\omega C} \quad (2.2)$$

$$f = \frac{\omega}{2\pi} = \frac{1}{2\pi\sqrt{LC}} \quad (2.3)$$

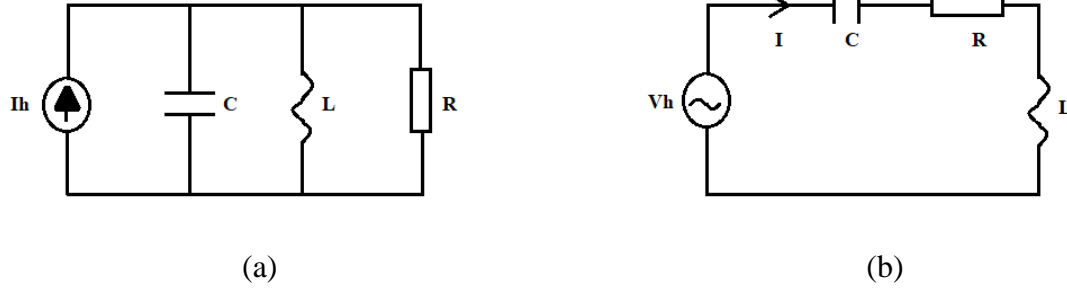


Figure 2.1 : (a) Parallel resonance circuit (b) Series resonance circuit.

2.2 Physical Approach to Ferroresonance

In linear circuits, resonance occurs when the capacitive reactance is equal to the inductive reactant at the frequency at which the circuit is driven (Serhat, et al., 2012). For ferroresonance circuits need iron core inductors that have a nonlinear property to have inductance values (Short, 2004). In a power system, ferroresonance occurs when a non-linear inductor is a feed from a series capacitor. The non-linear inductor in the power system may be caused by the magnetic core of the transformers or reactors in the transmission or distribution lines (Akinci, et al., 2012). The circuit capacitance in the power system can be caused by elements such as the following or during commissioning or deactivation of the transmission and distribution lines or circuit elements. (Endahl, 2017). Some examples of circuit capacitors elements grounding capacitance of the conductor, capacitance of bus bars, parallel line capacitance, capacitance in bushings.

In short, the effect of ferroresonance is a ferromagnetic material, in the system ferromagnetic materials are found in the cores of transformers or reactors (Short, 2004), (Valverde, 2012).

2.3 Nonlinear Magnetization Characteristic

The cores of the transformers are made of cold-rolled grain-oriented (CRGO) silicon steel. In order to prevent eddy losses in the core of the transformer, CRGO materials are produced and used in thicknesses ranging from 0.23 mm to 0.35 mm also cold rolled grain oriented steel is a ferromagnetic material.

The current characteristic versus voltage of a voltage transformer is usually known as the magnetic curve core of transformers design in knee area because when the core designed at a value higher than the elbow, goes into saturation. When the magnetic core is saturated, the magnetic core exhibits a characteristic that is different from the calculated or predictable, causing unpredictable oscillations in the system. \vec{B} is magnetic flux density it is seen in equation 2.6 and unit is Weber/m² or Tesla, A is area unit is m² is used in equation 2.7, \vec{H} is magnetic field intensity and the unit is A/m, N is the turn of the coil. μ magnetic permeability ($\mu_0 = 4\pi \cdot 10^{-7}$ H/m) the permeability is shown equality 2.4.

$$\mu = \mu_0 \cdot \mu_r \quad (2.4)$$

$$\oint \vec{H} \cdot d\vec{s} = I \quad (2.5)$$

$$\vec{B}(t) = \mu_0 \cdot \mu_r \cdot \vec{H} \quad (2.6)$$

$$U(t) = -N \frac{d}{dt} \int \vec{B}(t) \cdot d\vec{A} \quad (2.7)$$

The sinusoidal current I starts from zero and increases to the maximum point I_m . H increases in direct proportion to I , this is seen in equation 2.5. However, flux density B does not increase linearly in this increase. An example of hysteresis curve shown at figure 2.2.; as explained in figure follows the path 0A (Aydm, 2019). As the current decreases from I_m to 0, \vec{B} follows the path AB and remains at \vec{B}_r . \vec{B}_r called residual flux density (Jiles & Atherton, 1983). This time when the current is increased from zero to $-I_m$ the magnetic field strength increases to $-\vec{H}$ and following the path of flux, density BCD takes the value of $-B_m$. The HC value, where the flux density is zero, called the cleaning area (Lin, et al., 1989). Flux density follows path DEF when the magnetic field decreases to zero with current (Boduroglu, 1960), (Udpa & Lord, 1985), (Jiles, 1993). When the residual current starts in the second period, the flux density follows the fa path, not the 0A path. This loop named hysteresis loop (Allan & Moore, 2004). In other words, the curve does not close in the first period. (S.V.Kulkarni & S.A.Khaparde, 2004).

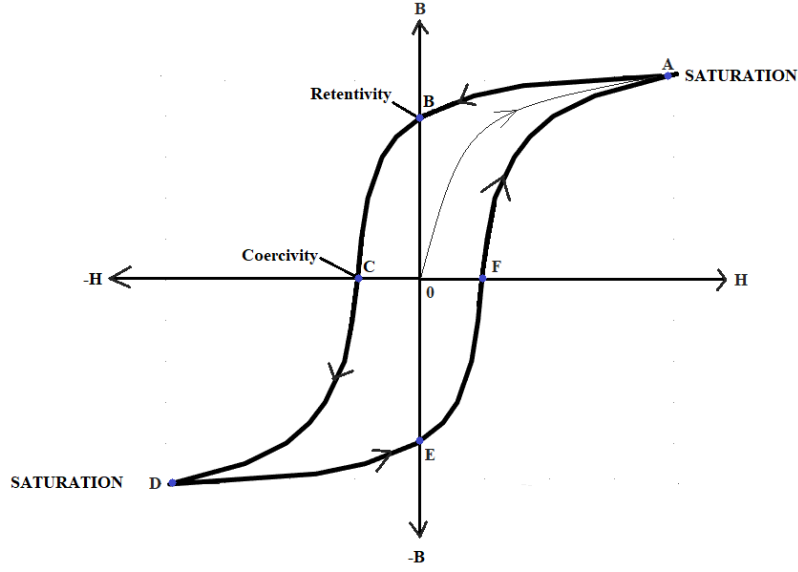


Figure 2.2 : Hysteresis curve (Patsios, et. al 2011).

2.4 Harmonics

Harmonics are high-frequency sine-shaped components of the fundamental frequency of the system. The frequencies of the harmonics, for example, when the basic frequency is 50 Hz, (50 Hz) x degree of harmonic. So 3rd Harmonic 150Hz, 5th Harmonic 250 Hz, 7th harmonic 350 Hz. figure 2.3 shows that one main signals with 3rd and 5th harmonic signals and signals with harmonics (Dandan, 2003). On sinusoidal function as seen equation 2.8 in other words, because there is no odd function, there are no cosine terms in Fourier expansion, there are only sinusoidal terms also this situation can be seen in figure 2.8. Therefore, only odd harmonics are formed (Rosa, 2006).

$$f(\omega t) = -f(-\omega t) \quad (2.8)$$

Calculation of harmonics by fourier analysis shown below equation 2.9;

$$f(t) = \frac{a_0}{2} + \sum_{n=1}^{\infty} (a_n \cos n\omega t + b_n \sin n\omega t) \quad (2.9)$$

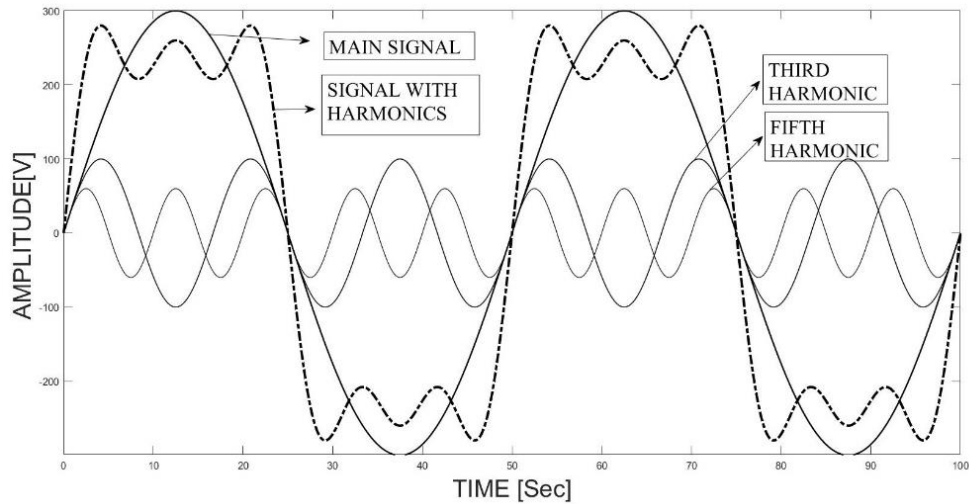


Figure 2.3 : Harmonics plot of the main signal, third and fifth signal and signals with harmonics.

Harmonics in the system can occur for many reasons. For example; Grooves in electrical machines, sudden load changes in synchronous machines, distortion of magnetic flux waveforms, magnetizing currents of transformers working in saturation zone, nonlinear loads in the network such as rectifier, inverter, welding machines. Also arc furnaces, voltage regulators, frequency inverters, engine speed control devices, energy transfer with high voltage direct current (HVDC), static volt-ampere reactive generators, uninterruptible power supply (UPS), effects of battery charging circuits, devices and methods used for energy saving

2.5 Subharmonics

The harmonics formed by dividing the main frequency by the main frequency in the system are called subharmonic. For example;

Network frequency f_0 : 50 Hz

Subharmonic oscillations, $f_0/2$: 25 Hz

Subharmonic oscillations, $f_0/3$: 16 $2/3$ Hz

Subharmonic oscillations, $f_0/5$: 10 Hz

Single subharmonics can be observed in ferroresonance events occurring in single-phase or three-phase systems, double subharmonics were observed only in ferroresonance events occurring in three-phase systems (Çetin, 2019).

2.6 Type of Ferroresonance

Electrical excitation that triggers the formation of ferroresonance in systems can be named as soft and hard excitation.

2.6.1 Soft excitation

When the system reaches ferroresonance conditions, used for oscillations where oscillation change is slow

2.1.6.1.a Steady state ferroresonance oscillations.

2.1.6.1.b Non-steady state increasing ferroresonance oscillations (Däumling & Hofstetter, 2018).

2.6.2 Hard excitation

Failures caused by saturation of the transformer core as a result of sudden changes such as a phase, phase earth or switching operations.

2.1.6.2.a: Steady-state ferroresonance oscillations

2.1.6. 2.b: Non-steady state increasing ferroresonance oscillations

2.1.6.2.c: Non-steady state decreasing ferroresonance oscillations (Däumling & Hofstetter, 2018).

2.7 Ferroresonance Waveforms

During the explanation ferroresonance waveforms, power system's period (T) depending on the systems frequency content, ferroresonant oscillations are normally classified.

2.7.1 Fundamental mode

Currents and voltage period are same period (T) with the system, fundamental mode has odd harmonics. Figure 2.4 is shown in fundamental mode graphs.

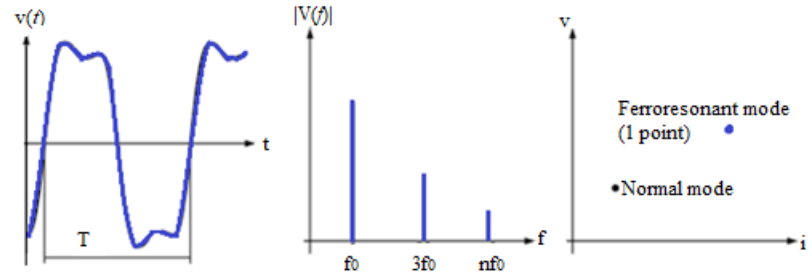


Figure 2.4 : Fundamentals mode graphs (Ferracci, 1998).

2.7.2 Subharmonic Mode

The sub-harmonic mode is the signal that involves the n times the system frequency signals (T/n) and also subharmonic frequency oscillations in. Figure 2.5 is shown in sub-harmonic mode graphs.

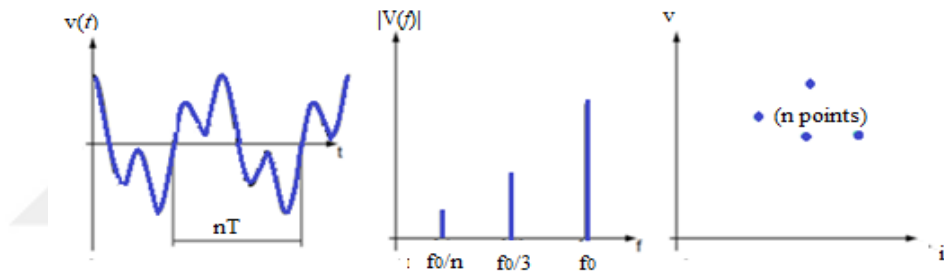


Figure 2.5 : Subharmonic Mode Graphs (Ferracci, 1998).

2.7.3 Quasi-Periodic Mode

This mode is not periodic. The spectrum is disorderly but it has a repetitious period. The frequency spectrums are impermanent identified as $nf_1 + mf_2$ where m and n are integers. Figure 2.6 is shown quasi-periodic mode graphs. (Valverde, 2012), (Ang, 2010).

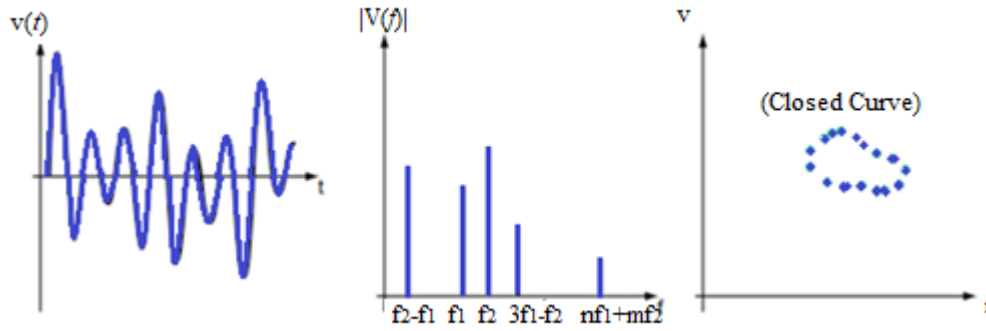


Figure 2.6 : Quasi-periodic mode graphs (Ferracci, 1998).

2.7.4 Chaotic Mode

The chaotic form differs than other forms; this form has not steady and not predictable form from other waveforms. Figure 2.7 is shown chaotic mode graphs.

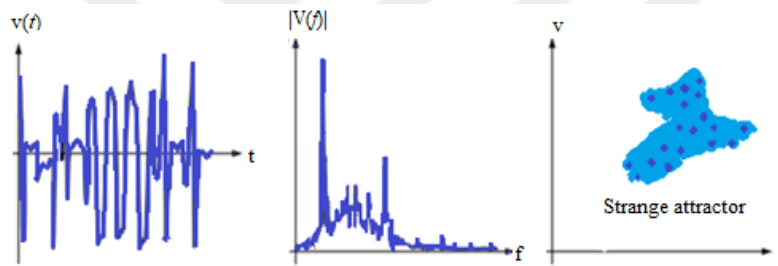


Figure 2.7 : Chaotic mode graphs (Ferracci, 1998).

2.8 Single Phase Ferroresonance Oscillation

In single-phase system, ferroresonance may happen the occasion of subharmonics. System capacitance and voltage transformer can cause ferroresonance formation. Figure 2.8 is shown single-phase non-resonance oscillation (Däumling & Hofstetter, 2018), (Chen, et al., 2012).

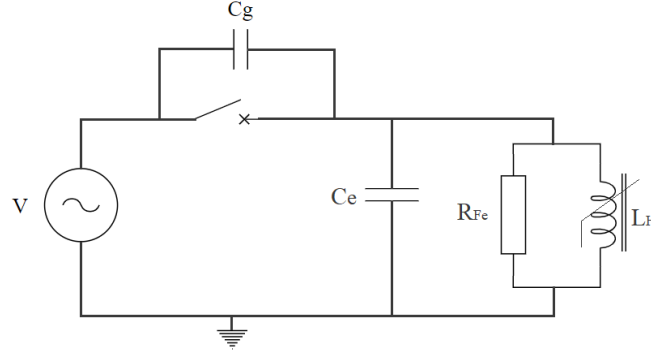


Figure 2.8 : Single-phase ferroresonance sample circuit.

A major circuit element is breakers that makeup capacitance in single-phase systems then overhead lines and capacitive load. C_g is capacitance of circuit breaker, L_H is non-linear main inductance of transformer coil, R_{Fe} is represent of non-linear resistance of transformer coil, C_e is total ground capacitance of facility.

2.9 Ferroresonance on Tree Phase System

All along many years, the three-phase ferroresonance was believed to be only difficulties of the transformer with non-grounding primary connections, as open delta, delta or ungrounded wye. However, the ferroresonance base on many other circumstance and motivation, for instance, transformer steel core saturation characteristic, type of transformer winding connection, residual fluxes density in the transformer iron core, initial conditions of the system, the circuit's capacitance, point-of-wave switching operation, total losses. So its predictability may be considered as quite complex and difficult (Mork, 2006), (Moses & Masoum, 2009).

When three-phase protective, switching are not used, possible that ferroresonance may appear. But a factor that may impact on it is not just limited to connection also to various constructive, operation, protective parameters and design. Thus Network characteristic, shunt capacitors, underground cables, transformer stray capacitance of circuit breakers, overhead conductors. The figure represent that three-phase circuit, which is ferroresonant, the circuit, can show that interrupting devices, three-phase transformer and overhead lines which represents by just capacitors. Ground connection represented by C_0 and connection phase to phase in wye connection C_1-C_0 . All inductive and resistive parameters are negligible. When two or one lines of switches

are closed for that cause where $C_1=C_0$ the transformer neutral must be ungrounded and circuit became ferroresonant circuit. Figure 2.9 shown possible ferroresonant circuit.

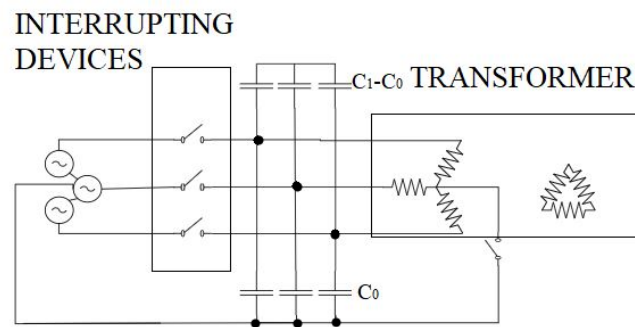


Figure 2.9 : Possible three phase ferroresonant circuit (Csanyi, 2020).

3. ARTIFICIAL NEURAL NETWORK

With the development of computer technology, mathematical and statistical methods can be analyzed with software tools. The application of computational and decision-making capabilities of the human brain to engineering analysis with the model approach started with the development of Artificial Neural Networks. With Artificial Neural Networks, it is possible to create trainable, self-learning, adaptive, decision making structures. Artificial Neural Networks can be applied to almost any discipline and offer very meaningful results. The artificial neural network is an artificial learning method created with inspiration from the biological neural network and whose mathematical expression is compared to biological neuron.

3.1 Biological Neuron

Since artificial neural networks based on biological models, the structure of a natural nerve cell must be understood before understanding artificial neural networks (Mishra & Srivastava, 2014), (Reed & MarksII, 1999). The figure 3.1 below shows a biological neuron. The biological neuron consists of a nucleus, soma and two types of appendages (Martinez, et al., 2012). One of them is dendrite, which is short and branched, also receives input information from other cells, and the other is axons, which is the structure that transmits the information in the long cell to other cells, that is, transmits the outputs. (Brink, et al., 2013). The combination of axon and dendrite is called a synapse (Lin, 2017), (Bose, 2001), (Watson, et al., 2010).

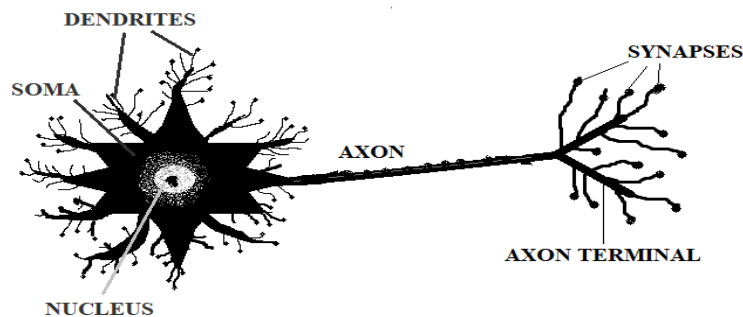


Figure 3.1 : Biological neuron (Watson, et al., 2010).

3.2 Modelling Neuron

The artificial neural network, the data to be learned in artificial neural networks entered as input. These input data can consist of data such as sound, image, voltage and picture. The artificial neural network performs learning by imitating the event that takes place in nerve cells and reveals the relationships between the cases. Inputs show as $X(n)$ while mathematical modelling of artificial neural networks is shown. Information processing is done when the inputs go to the middle layer. Inputs are values that are referred to as weight in mathematical modelling and are symbolized as $W(n)$, expressing the effect of the input set or another processing element in a layer before it on this process element (Mehrotra, et al., 2000). Weights can be positive or negative the input data is multiplied by a weight and summed with the bias value. The weights are randomly selected and may vary in the applied skew.

3.2.1 Single layer

The inputs are collected by multiplying them by the randomly assigned weight values according to the learning method chosen, as this explanation is equation 3.1. This summing process is symbolized by NET (Çakır, 2018) as equation 3.2. Addition of NET collection with b symbolized by bias, bias determines the neuron's response partner addition symbolized by V passes through the activation function and returns the output indicated by y . φ symbolized activation function as equation 3.5 while the matrix representation of the input information is the column, the weight values are shown in rows in the matrix. This is seen in equation 3.3 and 3.4. Epoch is the number of times weights are updated for possible inputs (Gurney, 2003), (Patel & Stonham, 1991), (Specht, 1991), (Huang & Xing, 2002), (Hassoun & Clark, 1988), (Sergio, et al., 2015).

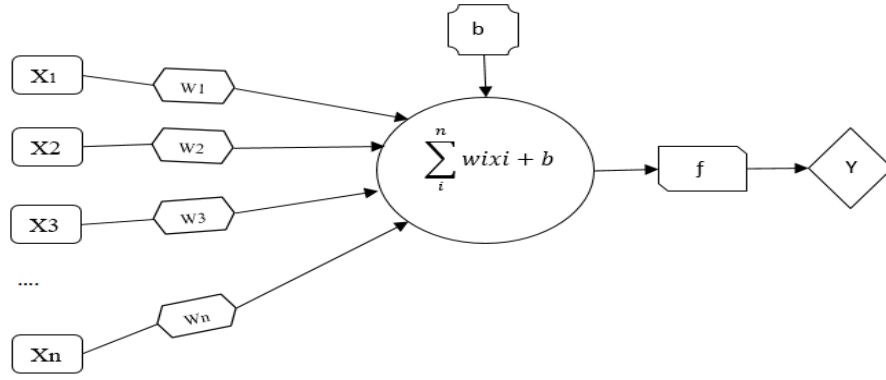


Figure 3.2 : Single layer artificial neural network (Sergio, et al., 2015).

$$v = (W_1 \times X_1) + (W_2 \times X_2) + (W_3 \times X_3) + \dots + (W_n \times X_n) + b \quad (3.1)$$

$$NET = \sum_{i=1}^n W_i \times X_i \quad (3.2)$$

$$X = \begin{bmatrix} X_1 \\ X_2 \\ X_3 \\ \dots \\ X_n \end{bmatrix} \quad (3.3)$$

$$W = [W_1 \ W_2 \ W_3 \ \dots \ W_n] \quad (3.4)$$

$$Y = \varphi(v) \quad (3.5)$$

3.2.2 Activation function

Many different activation functions can be used in artificial neural networks. Although the activation is not required in the function, it is expected that the output should not be linear, it can be differentiated, it does not have a lower and upper limit, it is monotonous increasing or decreasing, it converges at the origin point. Some examples of activation functions are as follows.

3.2.2.1 Linear (Purelin) function

This function has net input is produced exactly as output. It is linear, differentiable, has no upper and lower bounds, monotonous increasing and decreasing, converging at the origin point. Below figure 3.3 shows the linear function and mathematical equation of this function can show at equation 3.6.

$$x=y \quad (3.6)$$

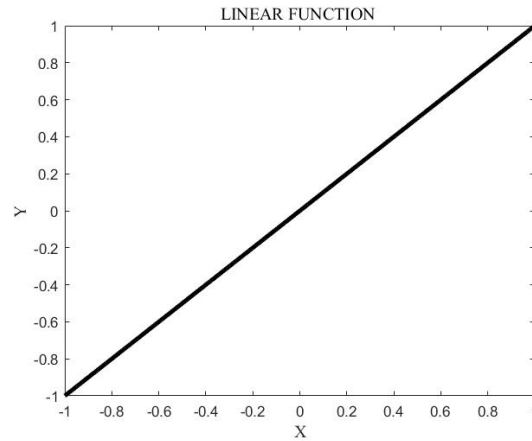


Figure 3.3 : Linear function.

3.2.2.2 Logsig (Sigmoid) function

Looking at the literature, one of the most applied activation functions is the sigmoid function. Sigmoid function is not linear, but modelling can be done by producing balanced outputs for both linear and nonlinear functions, it is differentiable, it has lower limit, upper limit, monotonous increasing and decreasing function. In figure 3.4 below sigmoid function can be seen. The equation 3.7 is a mathematical representation of the sigmoid function. (Karlik & Olgac, 2011), (Nguyen & Widrow, 1990).

$$f_{(NET)} = \frac{1}{1 + e^{-NET}} \quad (3.7)$$

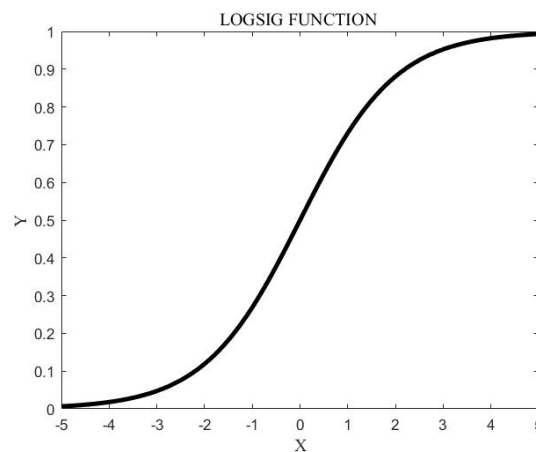


Figure 3.4 : Logsig function.

3.2.2.3 Hyperbolic tangent (Tansig) function

This is another most frequently used activation function in ANN. In order to use this function, input values normalized in the range -1 between 1, first, output values are also in this range increasing and decreasing, converges at the point of origin (Habibi & Jahani, 2017). In figure 3.5 below hyperbolic tangent (Tansig) function can be seen. The equation 3.8 is a mathematical representation of the tansig function.

$$f_{(NET)} = \frac{2}{1 + e^{-2 * NET}} - 1 \quad (3.8)$$

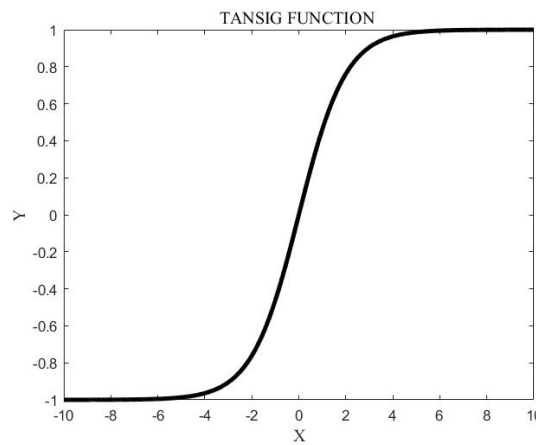


Figure 3.5 : Hyperbolic tangent (Tansig) function.

3.2.2.4 Hard sigmoid function

This function has a linear, differentiable, lower limit, upper limit features.

3.2.2.5 Softsign Function

Not linear, derivable, no lower limit, no upper limit, monotonous increasing and decreasing. Converges to itself at the point of origin Where $|x|$ = absolute value of the input. The soft sign usually using for regression computing problems. In figure 3.6 below soft-sign function can be seen. The equation 3.9 is a mathematical representation of the soft-sign function.

$$f_{(NET)} = \frac{NET}{|NET| + 1} \quad (3.9)$$

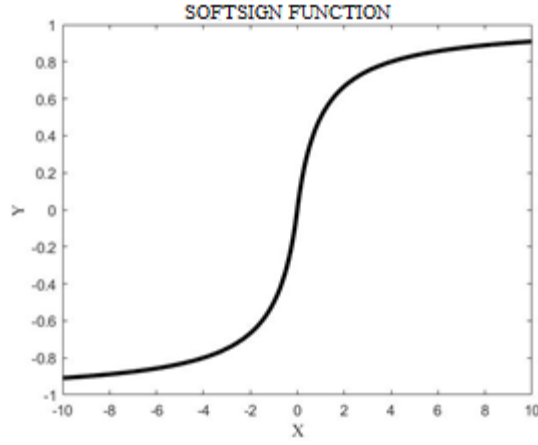


Figure 3.6 : Soft-sign function.

3.2.2.6 ReLU Function

This function has linear, differentiable, low limit, no upper limit, monotonous ascending and descending; antithetical converges to itself at the point of origin features (Habibi & Jahani, 2017). In the figure 3.7 below ReLU function can be seen. The equation 3.10 is a mathematical representation of the ReLU function.

$$f(NEt) = \begin{cases} 0 & \text{for } NEt < 0 \\ NEt & \text{for } NEt \geq 0 \end{cases} \quad (3.10)$$

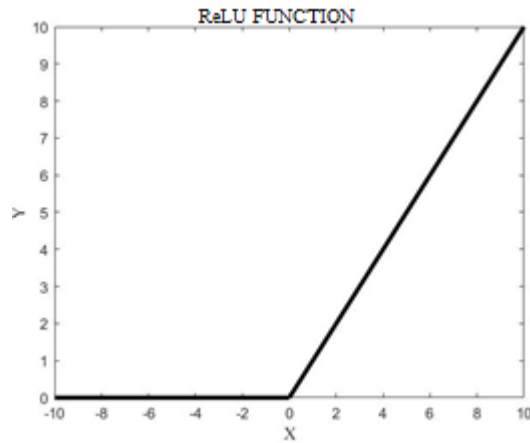


Figure 3.7 : ReLU function.

3.2.2.7 Softplus Function

This function has not linear, differentiable, has a lower limit, no upper limit, monotonous ascending and descending, do not converge at him at the point of origin features (Wang, et al., 2020). In figure 3.8 below soft-plus function can be seen. The equation 3.11 is a mathematical representation of the soft-plus function.

$$f(NEt)=\ln(e^{NEt} + 1) \quad (3.11)$$

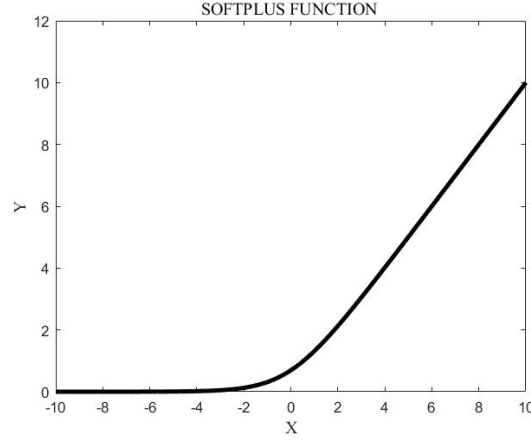


Figure 3.8 : Soft-plus function.

3.2.2.8 ELU Function

This function has not linear, derivable, no lower limit, no upper limit, monotonous increasing and decreasing, converges to itself at the origin point features (Basirat & Roth, 2019). In figure 3.9 below ELU function can be seen. The equation 3.12 is a mathematical representation of the ELU function. α is constant gradient (Normally, $\alpha=0.01$).

$$f(NEt) = \begin{cases} \alpha(e^{NEt} - 1) & \text{for } NEt < 0 \\ NEt & \text{for } NEt \geq 0 \end{cases} \quad (3.12)$$

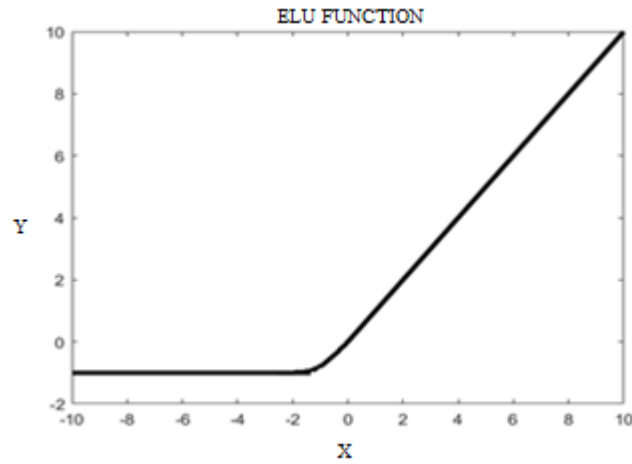


Figure 3.9 : ELU function.

3.2.2.9 Selu Function

This function has not linear, derivable, no lower limit, no upper limit, monotonous increasing and decreasing, converges to itself at the origin point features.

3.2.2.10 Swish Function

Not linear, derivable, has lower limit, no upper limit, monotonous increasing and decreasing, converges to itself at the origin point features.

3.2.2.11 Poslin Function

Positive linear Transfer Function is a positive linear function. If the net value is greater than zero and the net value is less than zero, it takes the value 0.

3.2.2.12 Step or Heaviside Function

Values with a threshold less than T will be zero. In figure 3.10 below step function can be seen.

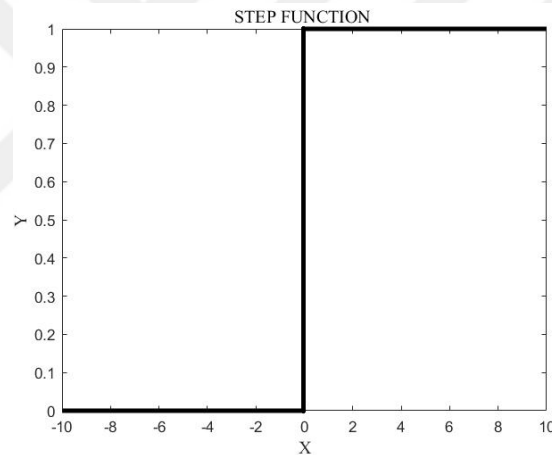


Figure 3.10 : Step function.

3.2.4 Multiple Layer

Unlike the single-layer system, the multi-layer system has hidden layers (Zhang & Morri, 1998). Each hidden layers outputs are inputs the other hidden layers inputs (Lippmann, 1987). A single layer, multiple layers has input data shown by X_n and outputs data shown by Y_n and between inputs and outputs multiple layer neural networks has hidden layer, the number of layers in the hidden layer can vary experimentally according to the method chosen and the most accurate learning (Park, et al., 1991).

Neurons in a layer are not related to each other and they perform the work of transferring the information that is in the system to the next layer or exit. Neurons in two layers in a row affect each other with different activation values and perform a transfer that determines the learning level of the mode figure 3.11 is shown multiple-layer figure (Zhang, et al., 1995).

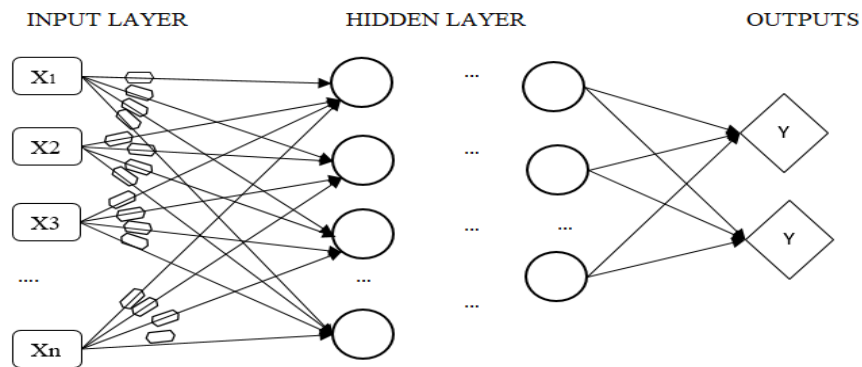


Figure 3.11: Multiple layers of artificial neural network.

3.3 Artificial Neural Network Models

There are two types of feed-forward and feed-back networks depending on the direction of the signal in the neural networks.

3.3 1 Feed Forward Neural Networks

In feed-forward ANN, cells are arranged in layers and the outputs of cells in one layer are given as input to the next layer via weights ANN, which is used to solve any problems, is as precise as the number of layers and the number of cells in the middle layer (Binev & Aires-de-Sousa, 2004), (Cybenko, 1996).

Despite undetermined information, besides areas such as object recognition and signal processing, feed-forward ANN is also widely used in the diagnosis and control of systems (Sazlı, 2006). Figure 3.12 is shown that feed-forward neural networks.

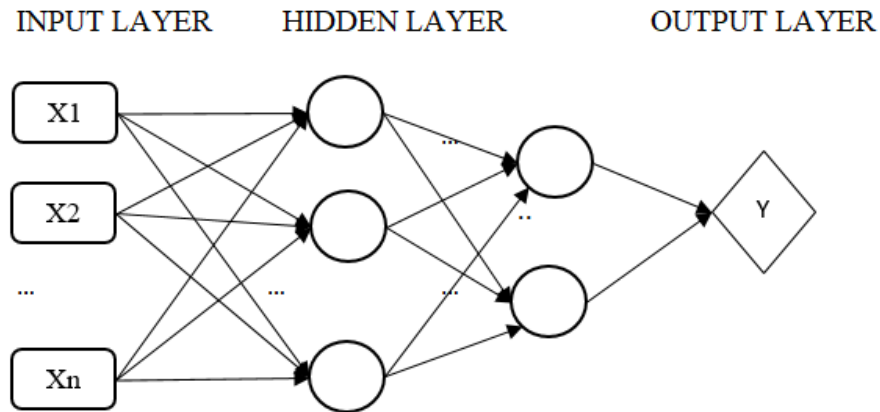


Figure 3.12 : Feed forward neural networks.

3 3 2 Feedback Neural Networks

In the feedback ANN, at least one cell is output as input to itself or other cells, and usually, feedback is done through a delay element. Feed-back can be between cells in a layer as well as cells between layers. Figure 3.13 is shown that Feed-back neural networks.

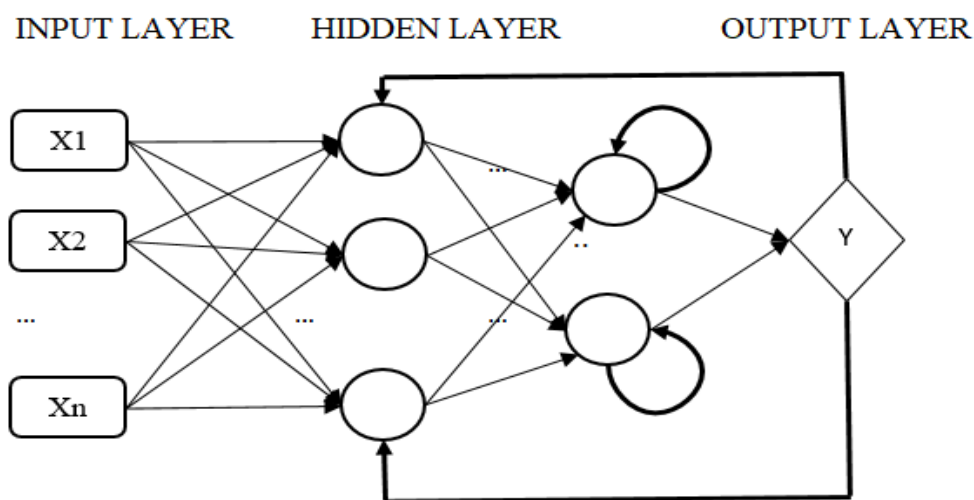


Figure 3.13 : Feed-back neural networks.

3 .4 Learning Rules in Artificial Neural Networks

Below are the information about Learning Rules in Artificial Neural Networks.

3.4.1 Error Correction Learning

It is the method used to train the error. With an algorithm such as the back-propagation algorithm, error values used to adjust the weights. If the system output is known to be

y and home, the output of the desired system can be shown as the error (e) = $k-y$. Error correction learning algorithms try to minimize the error signal in each training repeat (Komendantskaya, 2011), by doing this by adjusting the weight values. The most popular learning algorithm for this learning is the Gradient descent algorithm.

3.4.2 Self (Unsupervised) Learning

In this learning style, only sample inputs are given. No sample output information is given. The system is expected to learn the relationships between the parameters in the examples by itself (Kriesel, 2005). This is the learning method used mostly for classification problems. According to the information given in the introduction, the network creates its own rules so that each sample is classified among themselves.

3.4.3 Supervised Learning

During the training, an input and a target output vector are given to the system in pairs (Balaji & K.Baskaran, 2013), and the weight values in the system are updated and changed accordingly (Priddy & Keller, 2005).

3.4.4 Reinforcement Learning

This learning rule is a close method with a consultant. Instead of a learning to give the target output, there is no output to the artificial neural network, but a criterion that evaluates the goodness of the output obtained against the given input is used. Boltzman Rule or Genetic Algorithms developed by Hinton and Sejnowski are examples of reinforced learning to solve optimization problems (Sutton & Barto, 1998).

3.5 According to the learning time

Below is the information about the learning time.

3.5.1 Static

The ANN is trained with the training data and the structure of the network is recorded. The network always works with the same structure from now on. It does not change anything during its use (Fyfe, 2005).

3.5.2 Dynamic

After training of the ANN training data, it continues to regulate itself during its use, thus obtaining a constantly learning ANN.

3.6 Artificial Neural Network Advantages and Disadvantages

For detection ferroresonance in years researcher tried many difference method as power spectral density, current wavelet transform, short time Fourier transform and continuous wavelet transform. While these methods are basically determined by the statistical values of the frequencies, neural network method is a more dynamic determination method for nonlinear problems compared to these methods. ANN has obtained fame over alternative techniques, as it is a client in discovering relationships among large frames of data, to learn the certain status or operating condition of the objective schemes. (Pan & Chen, 2012). ANN has ability to work incomplete knowledge, has fault tolerance; corruption of one or higher cells of ANN does not prohibit it from engendering output. This feature makes the networks fault tolerance (Mijwil, 2018).

On the other hand it is created as a result of efficient algorithm an experience that works. There is no specific formula, the duration of the network is unidentified for example for this thesis NN27 duration was forty one minute, NN18 duration was one hour forty minutes.

It should not be ignored that the disadvantages of ANN networks, which are an ever-evolving science branch, are eliminated one by one and their advantages are widening day by day. This means that artificial neural networks will come an essential part of our lives increasingly relevant (Mijwil, 2018).

4. DATA ACQUISITION AND MODELLING

The overvoltages in this system can reach levels greater than 2.5 times the nominal voltage, and the ferroresonance event formed has a sinusoidal characteristic that is voltage-stressed. This property of voltage can be measured by harmonics and inter harmonics of the system. In this thesis, since the ferroresonance detection will be performed with ANN rather than the characteristic structure of the system, the signal characteristics have not been examined.

In figure 4.1, a schematic representation of the Seyitomer-Işıklar Electric Power transmission line transmission. It was created by using real parameters on the model given for the energy transmission line. As can be seen in the figure, ferroresonance scenarios were obtained by sudden cutting of the line by switching. As can be seen in the figure, ferroresonance scenarios were obtained by sudden cutting of the line by switching.

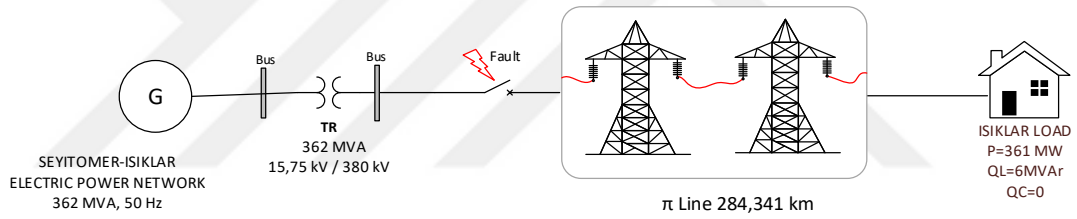


Figure 4. 1: Schematic representation of the transmission line.

The electrical parameters of the power plant and the line feeding the energy transmission line are given in table 4.1 below.

Table 4.1: Parameters of Electrical Components used in Seyitomer-Isıklr Power Networkfor Figure 4.1.

Electrical Components	Parameters
Generator	362 MVA, 15.75kV, 50Hz
Transformers	362 MVA, 15.75kV/380kV
Lengt of Line	284.341km
Load	P=361 MW Q _L =6MVAr

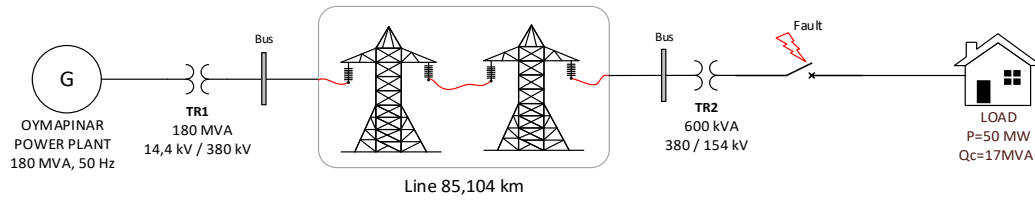


Figure 4. 2 : Schematic representation of the Oymapinar transmission line.

These different data were obtained from different branches on the line, and different time intervals were selected and different scenarios were created for Ann.

Table 4.2 : Parameters of Electrical Components used in Oymapinar Power Network for Figure 4.2.

Electrical Components	Parameters
Generator	180 MVA, 14.4 kV, 50 Hz
Transformers	TR1: 180 MVA, 14.4 kV / 380 kV TR2: 600 kVA, 380 kV / 154 kV
Lines	π Line(B1-B2): 85.104 km R: 0.2568 Ω /km L: 2e-3 H/km C: 8.6e-9 F/km Line(B2-B3): R: 1 Ω L: 1e-3 H
Loads	L1: P=50 MW, Qc=17 MVAR
Switch	S: 2.5 – 5 sec.- On 0 – 2.5 sec.- Off

4.1 Ferroresonance Detection

We have four signals calls as R1, R2, R3, and R4. Which inform below. In order to process these signals more easily, to capture the moment when they are ferroresonance, and to process the ferroresonance data, the data divided into 500 slices.

4.1.1 R1 Data

R1 has 49488 data. It divided into 98 pieces of 500 data. It is observed that ferroresonance started in part 62, figure 4.3 shows that when ferroresonance started in R1 data, mean is around 3-second failure started also this voltage change is visible in

figure 4.5. This ferroresonance form is chaotic form, heading 2.7.4 has information about chaotic ferroresonance.

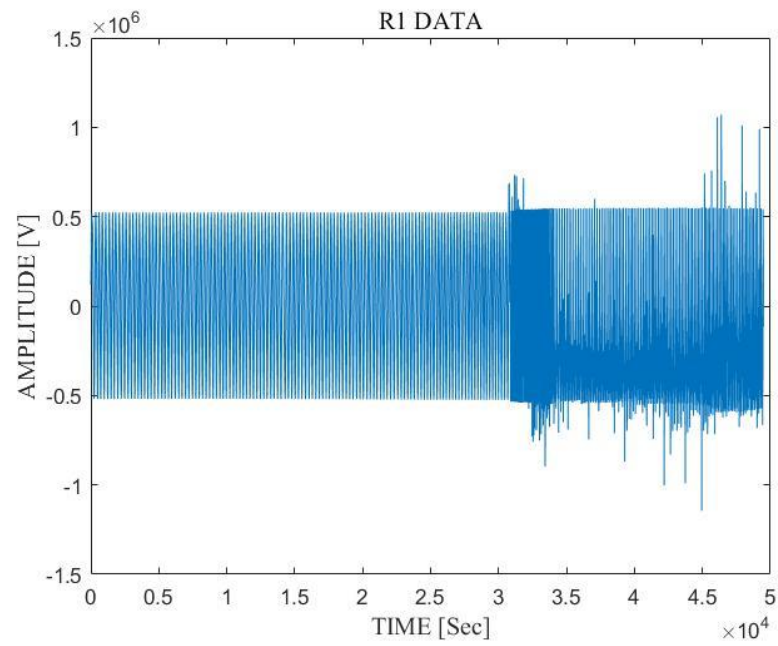


Figure 4.3: R1 data's plot.

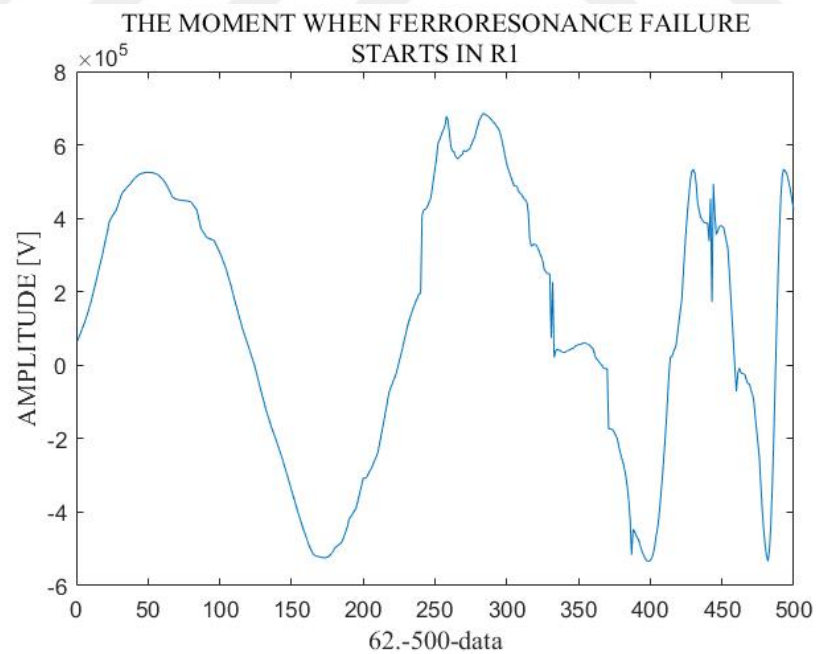


Figure 4.4 : The moment when ferroresonance failure started in R1.

4.1.2 R2 Data

R2 has 57005 data. It divided into 114 pieces of 500 data. It observed that ferroresonance started in part 57 figure 4.6 shown that starting point of ferroresonance. As shown figure 4.7, ferroresonance failure voltage magnitude of R2 data approximately 2.5×10^5 V. This kind of overvoltage failure can be dangerous for electrical equipment.

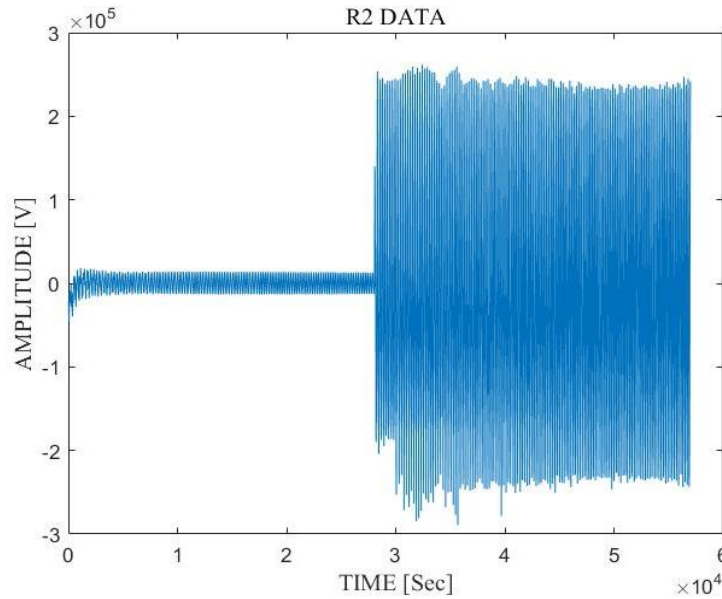


Figure 4.5 : R2 data.

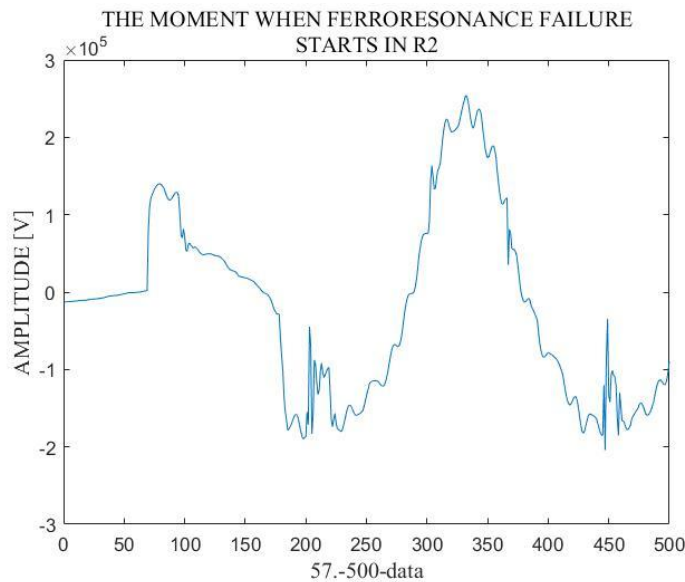


Figure 4.6 : The moment when ferroresonance failure started in R2.

4.1.3 R3 Data

R3 has 57005 data. It divided into 114 pieces of 500 data. We observed that ferroresonance started in part 57 figure 4.8 shown that beginning of ferroresonance fault, figure 4.9 shown that R3 data has over-voltage as R2 but the oscillation of R3 different than R2

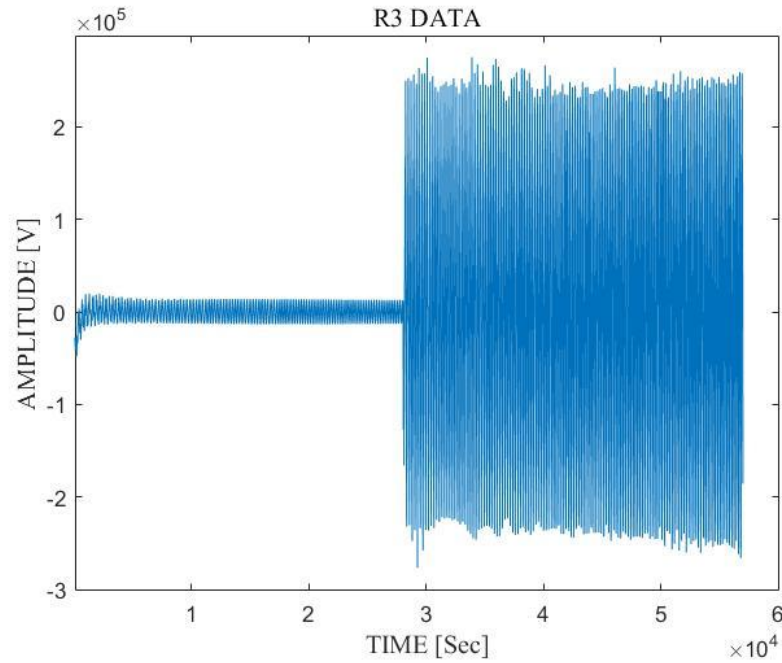


Figure 4.7 : R3 data.

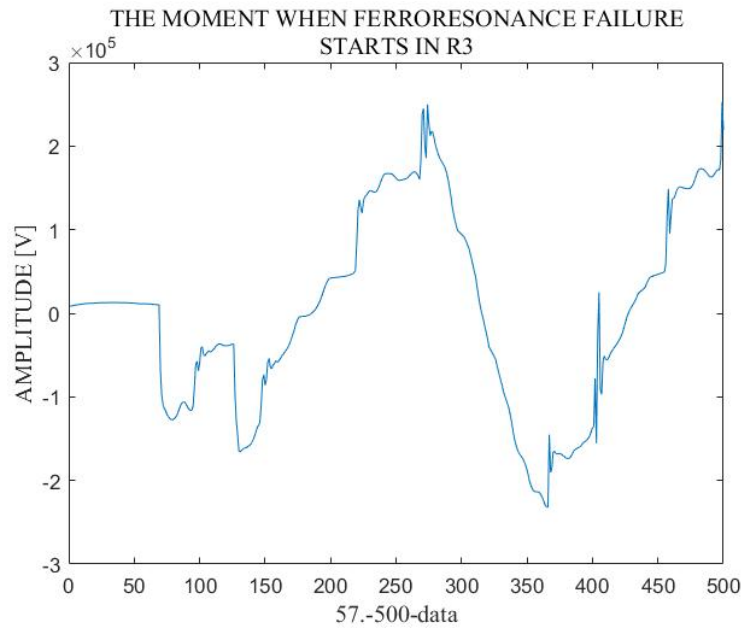


Figure 4.8 : The moment when ferroresonance failure started in R3.

4.1.4 R4 Data

R4 has 71054 data. It divided into 142 pieces of 500 data. It observed that ferroresonance started in part 29 shown in figure 4.11. Figure 4.10 shown R4 data which ferroresonance fault has overvoltage oscillation. This kind of oscillations can damage system equipment, which is on the same line with failure.

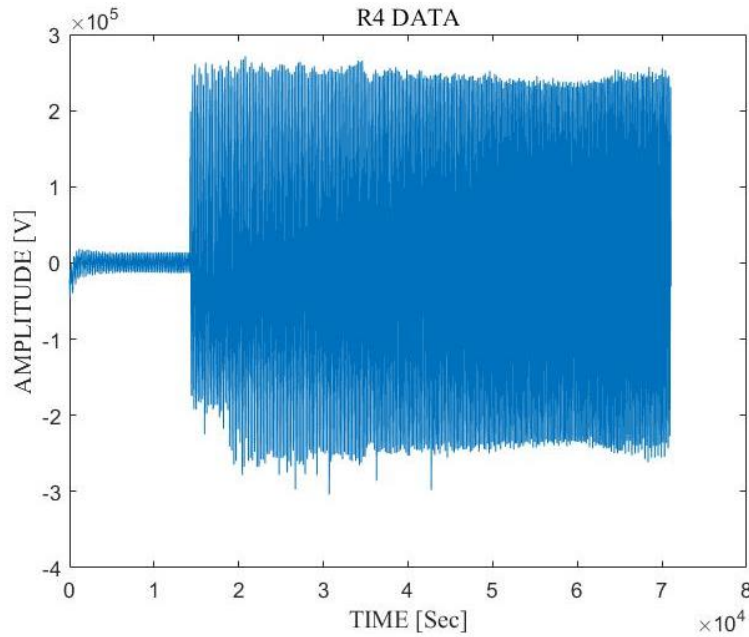


Figure 4.9 : R4 data.

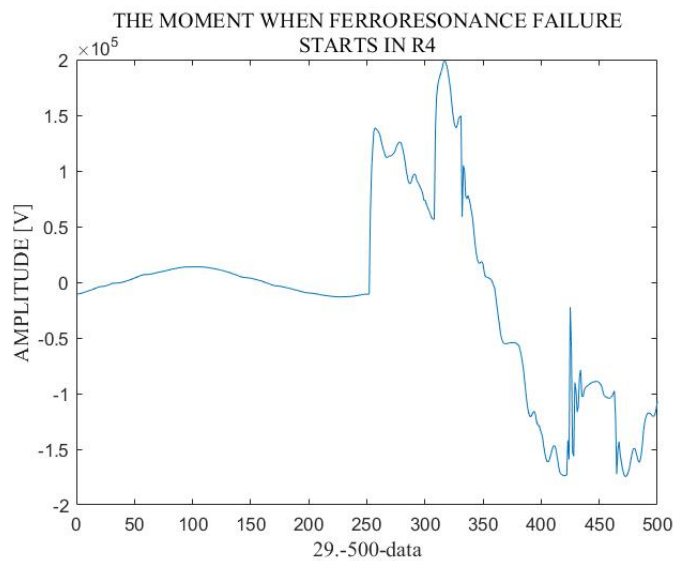


Figure 4.10 : The moment when ferroresonance failure started in R4.

5. APPLICATION OF ARTIFICIAL NEURAL NETWORK FOR FERRORESONANCE IDENTIFICATION

In this thesis, Turkey's energy transmission line Seyitomer-Isiklar and Oymapınar transmission line models were examined. In the analysis, firstly, the model of the transmission line was created by using the actual parameters on the Matlab-Simulink © model. Afterwards, the load parameters and synthetic faults were created on the Simulink model and the system was dragged into ferroresonance. Data on ferroresonance over voltages are collected ANN analyzes were performed and ferroresonance failures in the model were detected and separated. For the data created for the thesis study, the interface of the Matlab © tool used for created algorithm. Detailed analyzes of the variable parameters used in the study are also given in the appendix.

5.1 Matlab Tool

In this section, some variables in the algorithm will be mentioned. In this way, it will be easier for us to understand the results of the algorithm.

5.1.1 Variables

Figure 5.2 shown that the interface where input, target data entry, function etc. values are selected.

The image shows the 'Create Network or Data' dialog box in MATLAB. It has two tabs: 'Network' and 'Data'. The 'Network' tab is active. The dialog is divided into several sections:

- Name:** A text field labeled 'NETWORK NAME'.
- Network Properties:**
 - Network Type:** A dropdown menu set to 'Feed-forward backprop'.
 - Input data:** A dropdown menu set to '(Select an Input)'.
 - Target data:** A dropdown menu set to '(Select a Target)'.
 - Training function:** A dropdown menu set to 'TRAINLM'.
 - Adaption learning function:** A dropdown menu set to 'LEARNGDM'.
 - Performance function:** A dropdown menu set to 'MSE'.
 - Number of layers:** A text field set to '2'.
- Properties for:** A dropdown menu set to 'Layer 1'.
 - Number of neurons:** A text field set to '10'.
 - Transfer Function:** A dropdown menu set to 'TANSIG'.

At the bottom, there are buttons for 'View', 'Restore Defaults', 'Help', 'Create', and 'Close'.

Figure 5.1 : Variables input interface.

5.1.1.1 Network name

For identify network, it is used this section.

5.1.1.2 Network type

For this case, choose feed-forward back propagation other than this there are many network types as

Cascade-forward back-propagation, feed-forward distributed time delay, feed-forward time delay, generalized regression, Hopfield, Layer recurrent, Linear layer, Learning vector quantization (LVQ), Non-linear auto-regressive exogenous model (NARX), NARX series-parallel, perception, Probabilistic, Radial Basis (exact fit), Radial basis (fewer neurons), Self-organizing map (Demuth & Beale, 2004).

Back propagation is an algorithm method that calculates how weights and allegiances will change during network learning. Backpropagation steps basically; feed forward computation, to calculate output layer error, weights and bias update and output. (Rojas, 1996).

5.1.1.3 Input & train data

Here figure 5.2 form A to J we have variables. Input data and target data is the same it is ferroresonance data. Our input data is 13x500 matrix and our training data is 35x500 matrix.

5.7.1.4 Training function

Below table 5.1 shows that some training functions of *nnTool*. It is working with performance function as given chapter 5.7.1.6. These algorithms using for find optimizations algorithm and stop the process if calculations catch the minimum error value. There are many various optimization algorithms, which have a variety of different calculation and storage preconditions table 5.1 is options for using training algorithms in the table. The optimization algorithm detects how the arrangement of the frameworks in the neural network takes place.

Table 5.1: Training function table (Demuth & Beale, 2004).

Acronym	Algorithm	Description
LM	trainlm	Levenberg-Marquardt
BFG	trainbfg	BFGS Quasi-Newton
RP	trainrp	Resilient Backpropagation
SCG	trainscg	Scaled Conjugate Gradient
CGB	traingcb	Conjugate Gradient with Powell/Beale Restarts
CGF	traingcf	Fletcher-Powell Conjugate Gradient
CGP	traingcp	Polak-Ribière Conjugate Gradient
OSS	trainoss	One Step Secant
GDX	traingdx	Variable Learning Rate Backpropagation

Quasi-Newton method uses Hessian of loss function, conjugate gradient is performed forward with conjugate controls, which makes generally faster convergence than gradient descent directions. Train LM, Levenberg-Marquardt function, is common and most applied function in this tool also it is used in this thesis. Levenberg-Marquardt algorithm was developed to solve nonlinear least-squares problems. (Du & Stephanus, 2018) The Levenberg-Marquardt algorithm blends two minimization methods that are the gradient descent method and the Gauss-Newton method (Gavin, 2019), (Demuth & Beale, 2004).

5.7.1.5 Adaption Learning Function

For adaptation function program has two choices LEARNGD and LEARNGDM. LEARNGDM is used to calculate the change in weight using the input from the neuron and the error. (Siddique & Adeli, 2013). When momentum is not handled, the net can be installed at a regional minimum and oscillates. When momentum is used, it can gain the possibility of jumping. Momentum is between 0 and 1. If the momentum value is 0, the weight change is completely gradient dependent LEARNGDM is used in this thesis.

5.7.1.6 Performance Function

Three performance functions can be chosen; MSE mean is mean square error, other one is MSEREG which main is Mean squared error w/reg performance function which includes MSE one term proportional to modulus of the weights of ANN (Grassi, 2007/06/20) (Gao, et al., 2010) the last one is SSE and mean is sum square Error. In this thesis MSE and SSE used for performance function when training data. The first basic cost evaluation function. Equation 5.1 shown SSE mathematical representation and equation 5.2 shows the MSE function. In order to understand equality, where y_{pi} is actual value for the data point i , N is total number of data points, t_{pi} is predicted value for data point i . (Singh, et al., 2013).

$$SSE = \sum_{i=1}^N (t_{pi} - y_{pi})^2 \quad (5.1)$$

$$MSE = \frac{1}{N} \sum_{i=1}^N (t_{pi} - y_{pi})^2 \quad (5.2)$$

$$MAE = \frac{1}{N} \sum_{i=1}^N |xi - x| \quad (5.3)$$

5.7.1.7 Transfer Function

For transfer function, we have tree choices TANSİG, LOGSIG, PURELIN. These functions are mentioned in third chapter.

5.7.1.8 Performance

Plotted versus each of epochs for training in which the over training prevent while the MSE error for validation is at its min value (Hajian, 2018). An *epoch* refers to one cycle through the full training dataset.

5.7.1.9 Training state

In this plot, each window checks are plotted versus each *epochs*.

5.1.1.10 Regression

They show how much the input and output data overlap

5.2.Results of Training

The characteristics of the education groups classified in this section are explained. Five different groups and their features are explained. R1 divided into 98 pieces of 500 data. R1 of ferroresonance stars 62. 500 data and until 98. 500 data. R2 divided into 114 pieces of 500 data R2 of ferroresonance stars 57. 500 data till 114.500 data. R3 divided into 114 pieces of 500 data R3 of ferroresonance stars 57. 500 data and until 114. R4 divided into 142 pieces of 500 data. R4 of ferroresonance stars 29. 500 data and until 142. Input data, target data and created using data pieces as mentioned chapter 3. Input, target and example data created using this ferroresonance data from four-failure period used as input and target on

5.2.1 First group of training

For first group training chosen network type feed-forward back-propagation, for training function preferred *trainlm*, *learngdm* is chosen as adaptation learning function, for performance function MSE and transfer function TANSIG, for epochs 1000, and max fails 1000 table 5.2 show that group's information. Some examples of training below, Here are a few examples of this training group, not all of them are included. The rest is in the appendix.

5.2.1.1 NN28

For NN28 neuron number is 20. We can see figures performance of NN28. Figure 5.2 shown that performance output of NN28 and figure 5.3 shown that regression output of NN28 training. Figure 5.2 plot shows that the network training has stopped at the 209th iteration but it has concluded the best performance at the 9th iteration. For figure 5.3 output data match with target data 0,99459 this matches shows us the training is successful.

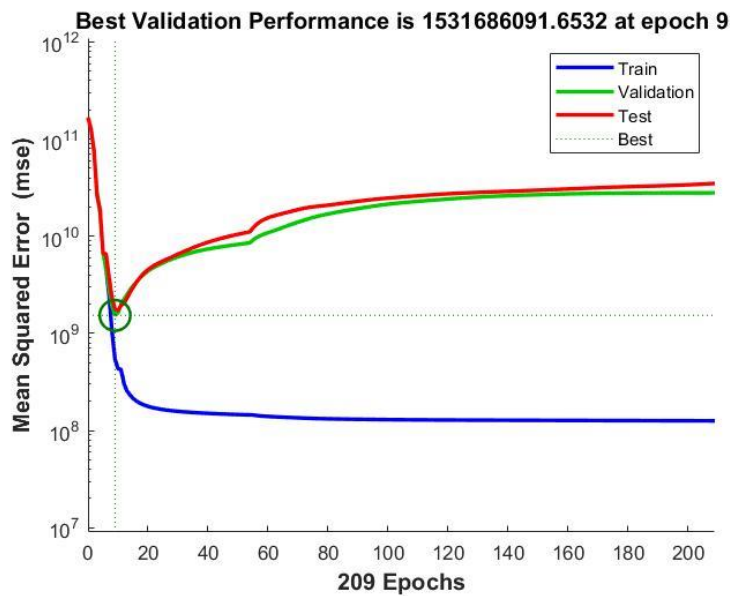


Figure 5.2 : Performance plot for NN28.

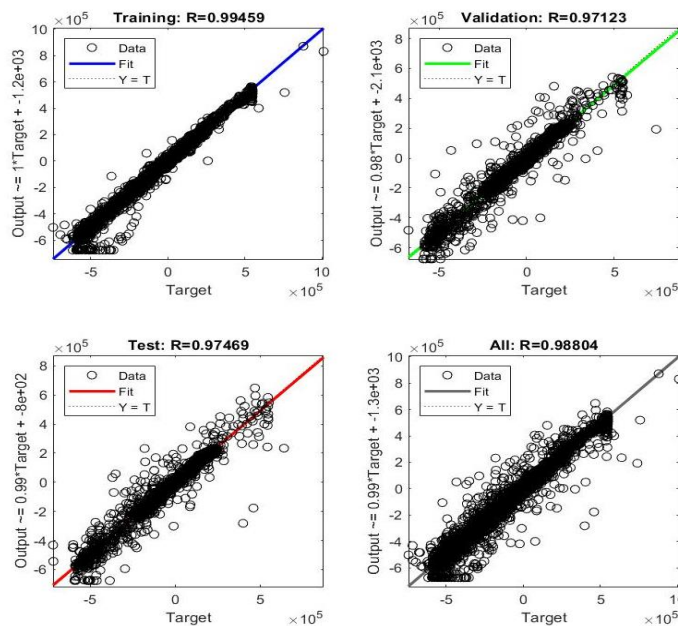


Figure 5.3 : Regression plot for NN28.

5.2.1.2 NN11

For NN11 neuron number is 35. The figure 5.4 shown that performance output of NN11 and figure 5.5 shown that regression output of NN11 training. In the chart, the network training has ended at the 1000th iteration but it has acquired the best performance on the 28th, best performance value is 3884189436,99. The regression output for 35 neuron of first training group input and target data match 0,98113.

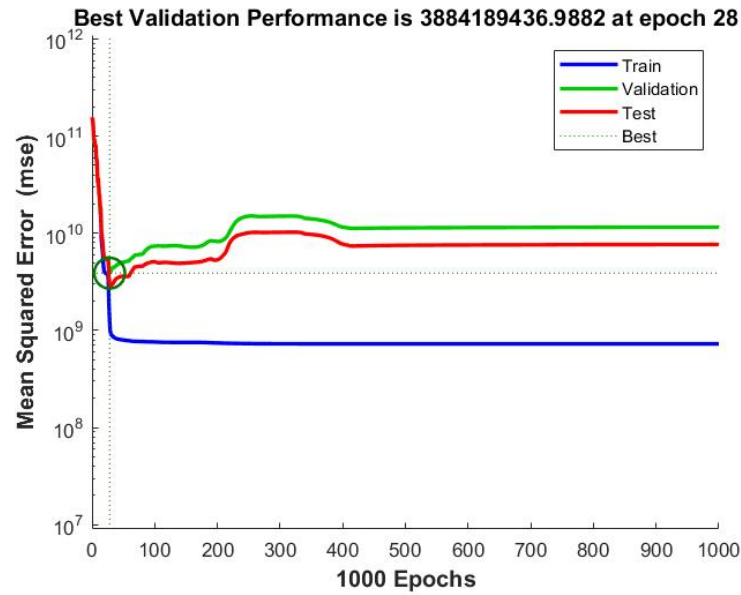


Figure 5.4 : Performance plot for NN11.

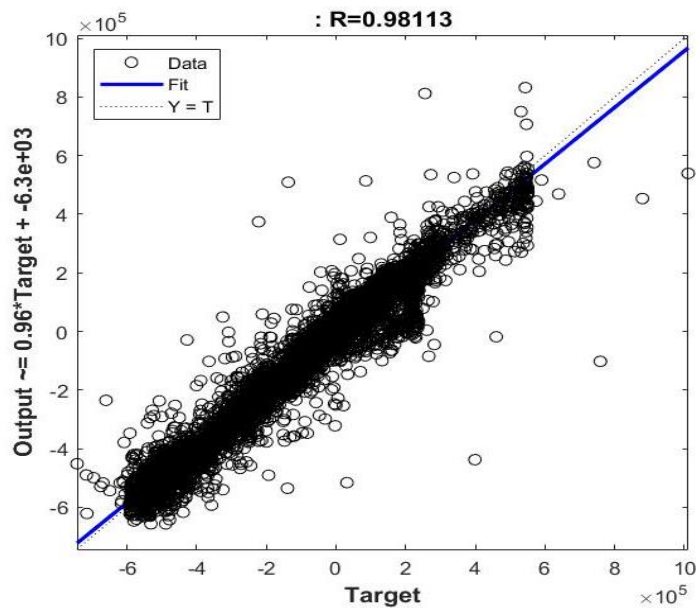


Figure 5.5 : Regression plot for NN11.

5.2.1.3 NN12

For NN12 for neuron number is 50. Figure 5.6 shown that performance output of NN12 and in the chart, the network training has ended at the 1000th iteration but it has acquired the best performance on the 6th. The regression output of 50 neuron of first training group input and target data match 0,99576 figure 5.7 shown that regression output of NN12 training.

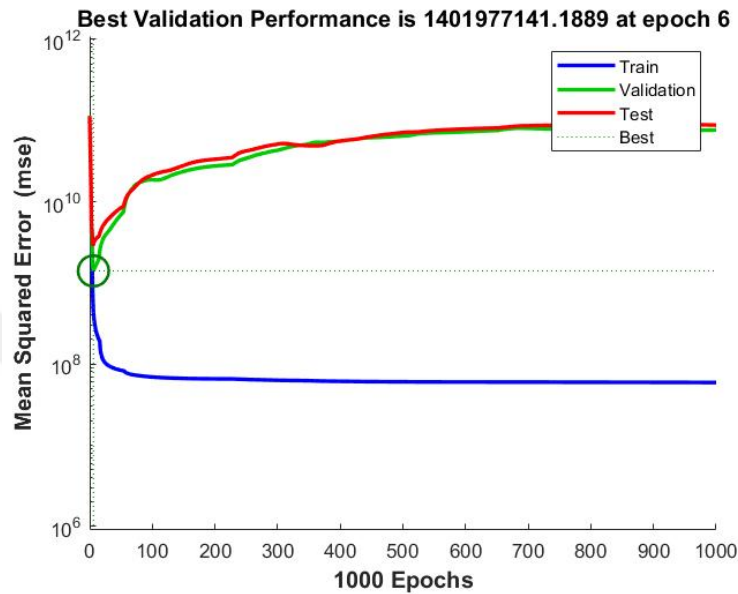


Figure 5.6 : Performance plot for NN12.

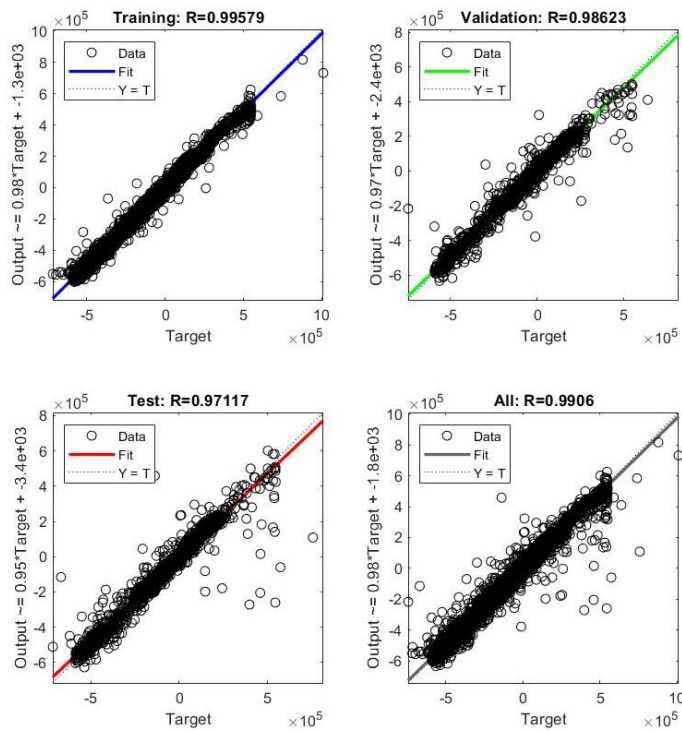


Figure 5.7 : Regression plot for NN12.

Table 5.2 : First Group of Training.

NETWORK NAME	NETWORK TYPE	TRAINING FUNCTION	ADAPTATION LEARNING FUNCTION	PERFORMANCE FUNCTION	NUMBER OF LAYERS	NUMBER OF NEURONS	TRANSFER FUNCTION	EPOCHS	MAX FAIL	REGRESSION
NN7	fbc	trainlm	learngdm	MSE	2	2	TANSIG	1000	1000	0.27793
NN23	fbc	trainlm	learngdm	MSE	2	5	TANSIG	1000	1000	0.96002
NN8	fbc	trainlm	learngdm	MSE	2	10	TANSIG	1000	1000	0.98113
NN31	fbc	trainlm	learngdm	MSE	2	15	TANSIG	1000	1000	0.99306
NN28	fbc	trainlm	learngdm	MSE	2	20	TANSIG	1000	1000	0.99459
NN11	fbc	trainlm	learngdm	MSE	2	35	TANSIG	1000	1000	0.99592
NN12	fbc	trainlm	learngdm	MSE	2	50	TANSIG	1000	1000	0.98554

5.2.2 Second Group of Training

For second group training chosen network type feed-forward back-propitiation, for training function preferred *trainlm*, *learnngdm* is chosen as adaptation learning function, for performance function MSE and transfer function TANSIG, for epochs 1000, and max fails 500 table 5.3 shown that group's information. Some examples of training below, Here are a few examples of this training group, not all of them are included. The rest is in the appendix.

5.2.2.1 NN18

For NN18 is neuron number 20. Figure 5.8 shown that performance output of NN18 in the chart, the network training has ended at the 506th iteration but it has acquired the best performance on the 6th. The regression output 20 neuron for second training group input and target data match 0,9943 and figure 5.9 shown that regression output of NN18 training.

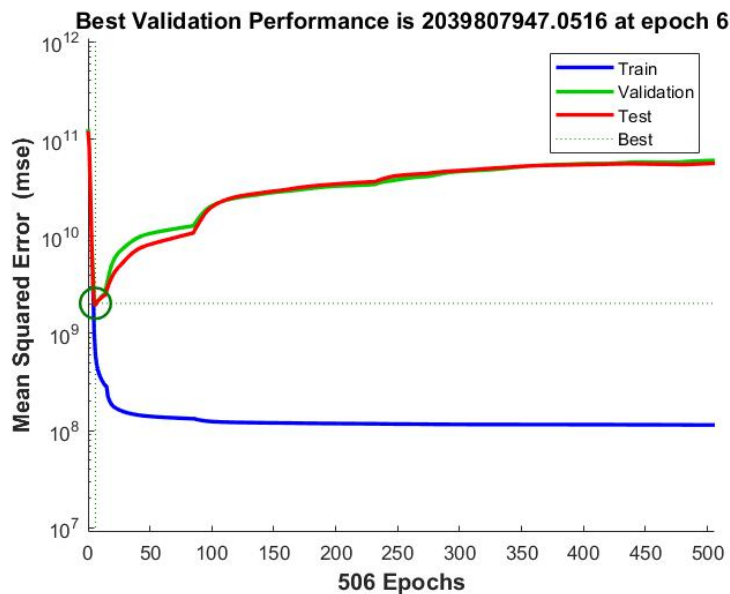


Figure 5.8 : Performance plot for NN18.

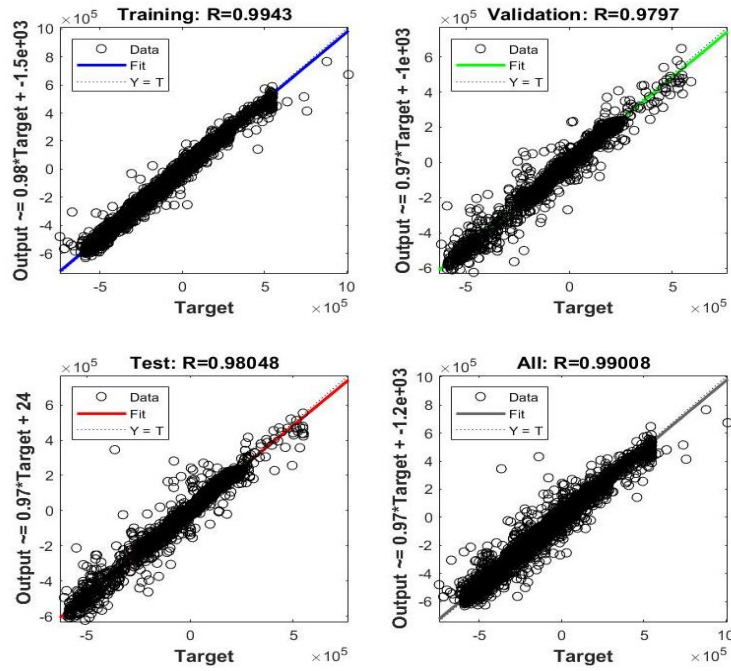


Figure 5.9 : Regression plot for NN18.

5.2.2.2 NN24

For NN24 is neuron number 35. Figure 5.10 shown that performance output of NN24 in the chart, the network training has ended at the 515th iteration but it has acquired the best performance on the 15th. The regression output 35 neuron for second training group input and target data match 0,99752 and figure 5.11 shown that regression output of NN24 training.

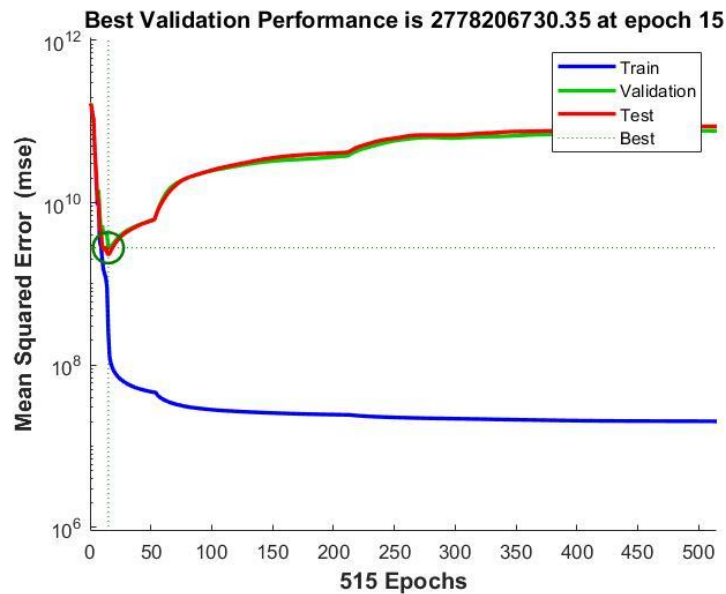


Figure 5.10 : Performance plot for NN24.

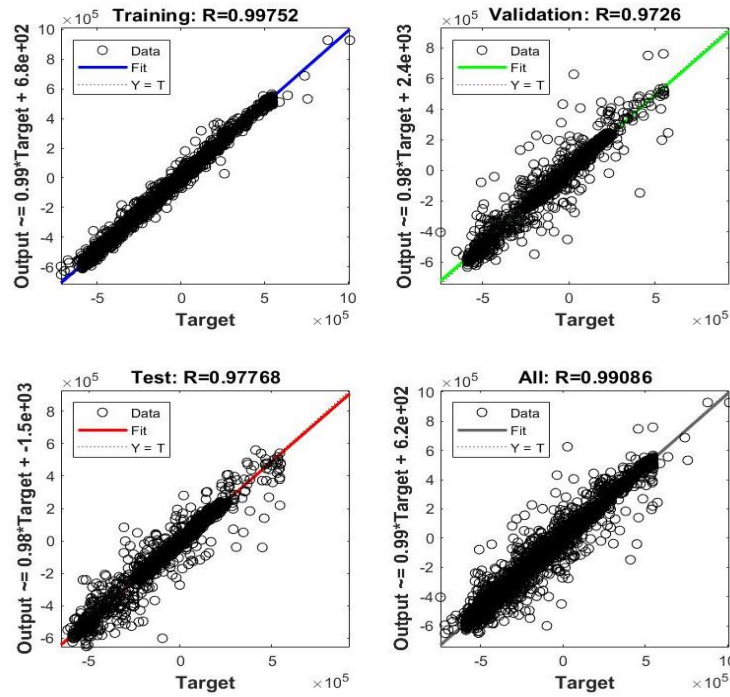


Figure 5.11 : Regression plot for NN24.

5.2.2.3 NN6

For NN6 neuron number is 50. The figure 5.12 shown that performance output of NN6 in the chart, the network training has ended at the 510th iteration but it has acquired the best performance on the 10th. The regression output 50 neuron for second training group input and target data match 0,99279 and figure 5.13 shown that regression output of NN6 training.

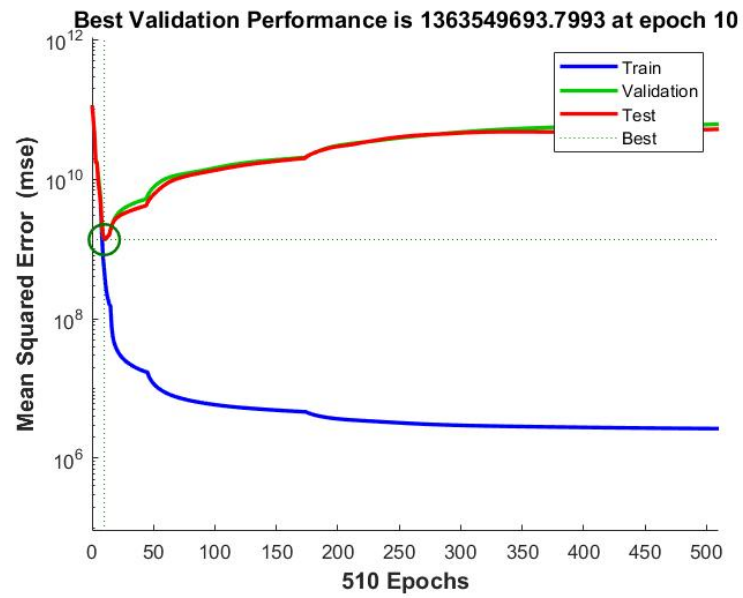


Figure 5.12 : Performance Plot for NN6.

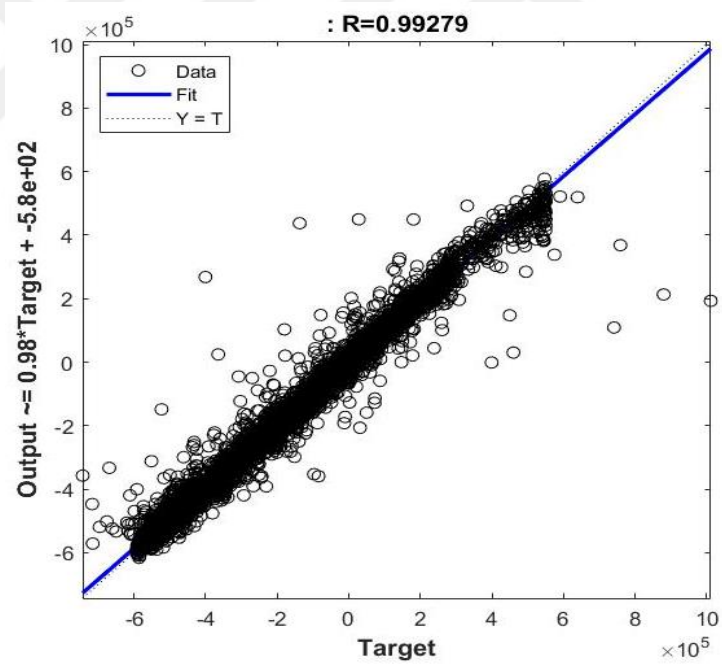


Figure 5.13 : Regression plot for NN6.

Table 5.3 : Second Group of Training.

NETWORK NAME	NETWORK TYPE	TRAINING FUNCTION	ADAPTATION LEARNING FUNCTION	PERFORMANCE FUNCTION	NUMBER OF LAYERS	NUMBER OF NEURONS	TRANSFER FUNCTION	EPOCHS	MAX FAIL	REGRESSION
NN4	fbc	trainlm	learngdm	MSE	2	2	TANSIG	1000	500	0.52888
NN22	fbc	trainlm	learngdm	MSE	2	5	TANSIG	1000	500	0.77428
NN5	fbc	trainlm	learngdm	MSE	2	10	TANSIG	1000	500	0.98554
NN17	fbc	trainlm	learngdm	MSE	2	15	TANSIG	1000	500	0.99306
NN18	fbc	trainlm	learngdm	MSE	2	20	TANSIG	1000	500	0.99430
NN24	fbc	trainlm	learngdm	MSE	2	35	TANSIG	1000	500	0.99752
NN6	fbc	trainlm	learngdm	MSE	2	50	TANSIG	1000	500	0.99279

5.2.3 Third Group of Training

For third.group training choosen network type feed forward backprop for training function preferred *trainlm,learnngdm* is chosen as adaptation learning function,for performance function MSE and transfer function TANSIG,for epochs 1000,and max fail 200 table 5.4 shown that group's information. Some examples of training below, Here are a few examples of this training group, not all of them are included. The rest is in the appendix.

5.2.3 1 NN29

For NN29 neuron number is 35. The figure 5.14 shown that performance output of NN29 and figure 5.15 shown that regression output of NN29 training.at the graph for performance NN29 training stopped at the 1000th iteration but it has acquired the best performance on the 21th. The regression output of 35 neuron of fourth training group input and target data match 0,99635.

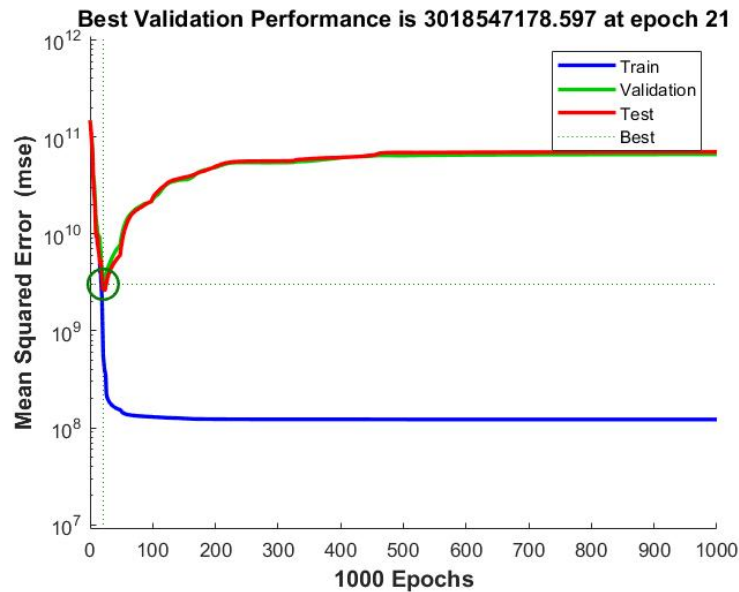


Figure 5.14 : Performance plot for NN29.

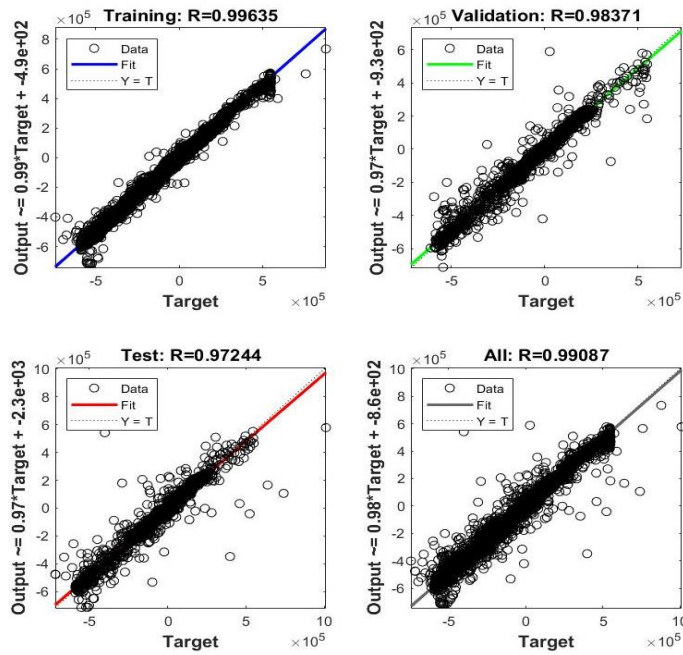


Figure 5.15 : Regression plot for NN29.

5.2.3 2 NN30

For NN30 neuron number is 50. The figure 5.16 shown that performance output of NN30 at the graph for performance NN30 training stopped at the 213th iteration but it has acquired the best performance on the 13th. The regression output of 50 neuron of third training group input and target data match 0,9901. and 5.17 shown that regression output of NN30 training.

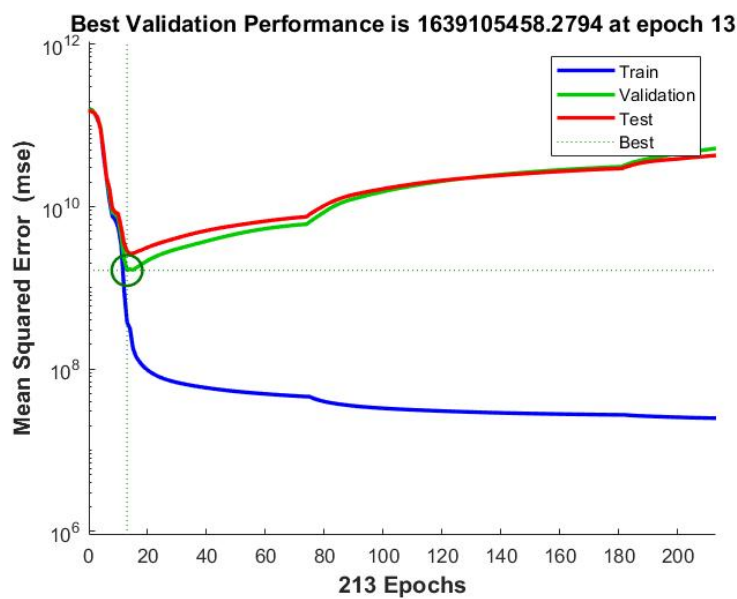


Figure 5.16 : Performance plot for NN30.

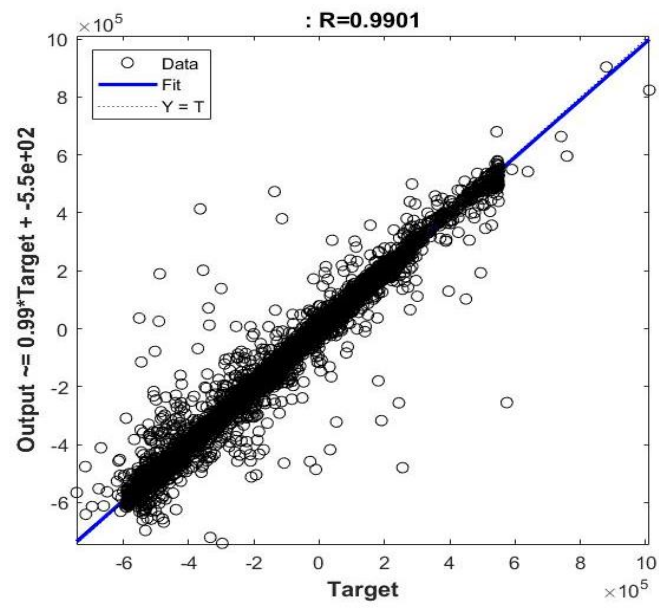


Figure 5.17 : Regression plot for NN30.

Table 5.4 : Third group of training.

NETWORK NAME	NETWORK TYPE	TRAINING FUNCTION	ADAPTATION LEARNING FUNCTION	PERFORMANCE FUNCTION	NUMBER OF LAYERS	NUMBER OF NEURONS	TRANSFER FUNCTION	EPOCHS	MAX FAIL	REGRESSION
NN20	fbc	trainlm	learngdm	MSE	2	2	TANSIG	1000	200	0.58136
NN21	fbc	trainlm	learngdm	MSE	2	5	TANSIG	1000	200	0.95854
NN25	fbc	trainlm	learngdm	MSE	2	10	TANSIG	1000	200	0.99045
NN26	fbc	trainlm	learngdm	MSE	2	15	TANSIG	1000	200	0.99615
NN27	fbc	trainlm	learngdm	MSE	2	20	TANSIG	1000	200	0.99477
NN29	fbc	trainlm	learngdm	MSE	2	35	TANSIG	1000	200	0.99635
NN30	fbc	trainlm	learngdm	MSE	2	50	TANSIG	1000	200	0.99010

5.2.4 Fourth Group of Training

For fourth group training chosen network type feed forward *backprop*, for training function preferred *trainlm*, *learngdm* is chosen as adaptation learning function, for performance function SSE and transfer function *tansig*, for epochs 1000, and max fail 500 table 5.5 shown that group's information. This group training could not success for our ferroresonance data. When regression output between 0 and -1 means the higher level of error for this domain of data train and test are very much larger than the error value for validation second group of training of table 5.3 can be shown below.

5.2.5 Fifth Group of Training

For fourth group training chosen network type feed forward *backprop*, for training function preferred *trainlm*, *learngdm* is chosen as adaptation learning function, for performance function MSE and transfer function *logsig* for epochs 1000, and max fail 1000 table 5.6 shown that group's information. This group training could not as successful as transfer function *tansig* for our ferroresonance data.

Table 5.5 : Fourth group of training.

NETWORK NAME	NETWORK TYPE	TRAINING FUNCTION	ADAPTATION LEARNING FUNCTION	PERFORMANCE FUNCTION	NUMBER OF LAYERS	NUMBER OF NEURONS	TRANSFER FUNCTION	EPOCHS	MAX FAIL	REGRESSION
NN1	fbc	trainlm	learngdm	SSE	2	2	TANSIG	1000	500	0.13512
NN15	fbc	trainlm	learngdm	SSE	2	5	TANSIG	1000	1000	0.0778
NN2	fbc	trainlm	learngdm	SSE	2	10	TANSIG	1000	500	0.225
NN3	fbc	trainlm	learngdm	SSE	2	50	TANSIG	1000	500	-0.059251

Table 5.6 : Fifth group of training.

NETWORK NAME	NETWORK TYPE	TRAINING FUNCTION	ADAPTATION LEARNING FUNCTION	PERFORMANCE FUNCTION	NUMBER OF LAYERS	NUMBER OF NEURONS	TRANSFER FUNCTION	EPOCHS	MAX FAIL	REGRESSION
NN13	fbc	trainlm	learngdm	MSE	2	10	LOGSIG	1000	1000	0.78735
NN14	fbc	trainlm	learngdm	MSE	2	15	LOGSIG	1000	1000	0.86119
NN32	fbc	trainlm	learngdm	MSE	2	20	LOGSIG	1000	1000	0.75319
NN33	fbc	trainlm	learngdm	MSE	2	35	LOGSIG	1000	1000	0.99636
NN34	fbc	trainlm	learngdm	MSE	2	50	LOGSIG	1000	1000	0.97117



6. CONCLUSION

In this study, using the actual parameters have been created using Turkey's Seyitömer-Işıklar energy transmission line model. The main purpose is to observe the algorithms created in artificial neural networks using ferroresonance voltage values, which is a nonlinear condition used as input of artificial neural network. In the algorithms created, the contribution of the variables to the successful result was examined and the results of the algorithms were compared. Changes were made on the number of layers; transfer function, performance function and max fail variables. The created algorithms can be examined in detail in chapter 5.2. The results of the algorithms created, their success and comparison are given below. Below is figure 6.1. the number of layers and learning graph used in the first education group, figure 6.2. the number of layers and learning graph used in the second education group, figure 6.3. the number of layers and learning graph used in the third education group, the effect of the transfer function used in this research on success was obtained by comparing the fourth training group and the first training group.

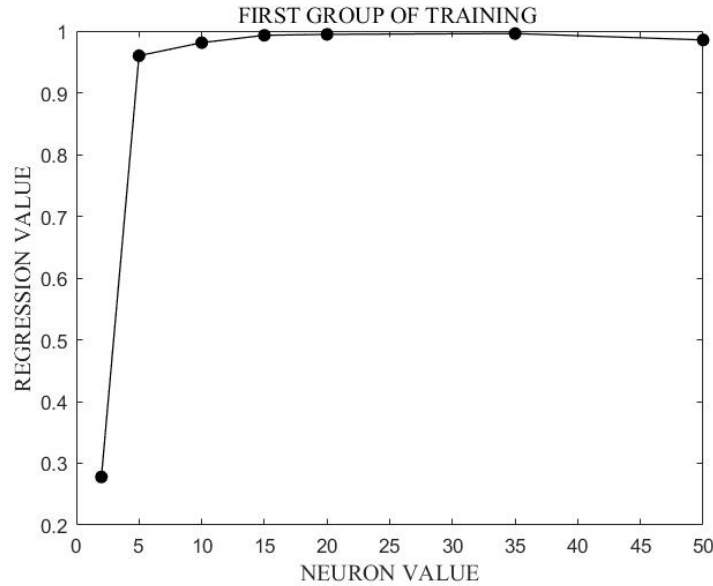


Figure 6.1 : First group of training graph.

Figure 6.2, it was created by using regression and neuron numbers from the information given in Table 5.3.

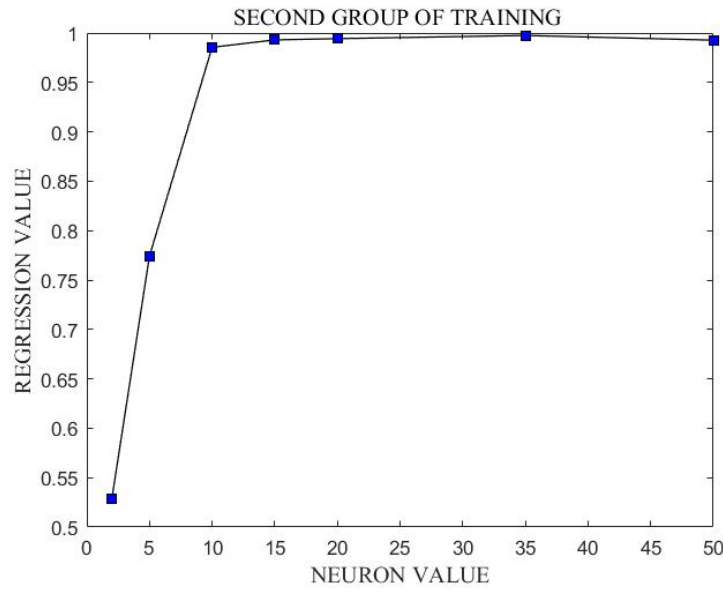


Figure 6.2 : Second group of training graph.

Figure 6.3, it was created by using regression and neuron numbers from the information given in Table 5.4.

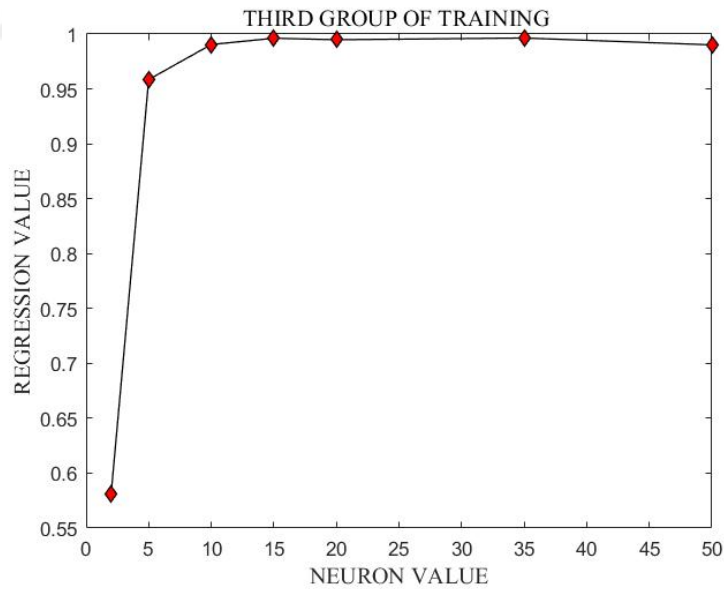


Figure 6.3 : Third group of training graph.

First, second, third group function, *tansig* function has provided more successful learning with fewer layers. When *tansig* function is successful, when we examine the number of layers; while there was not much difference in the learning results of 20-35

layers, it was observed that the learning level decreased between 35-50 layers. Since the increase in the number of layers means an increase in the analysis process, it has been observed that the most optimal learning is third training group's 10th layer because the number of failures also affects the process. As can be seen from the obtained results, this proposed algorithm has been very successful in detecting malfunctions.

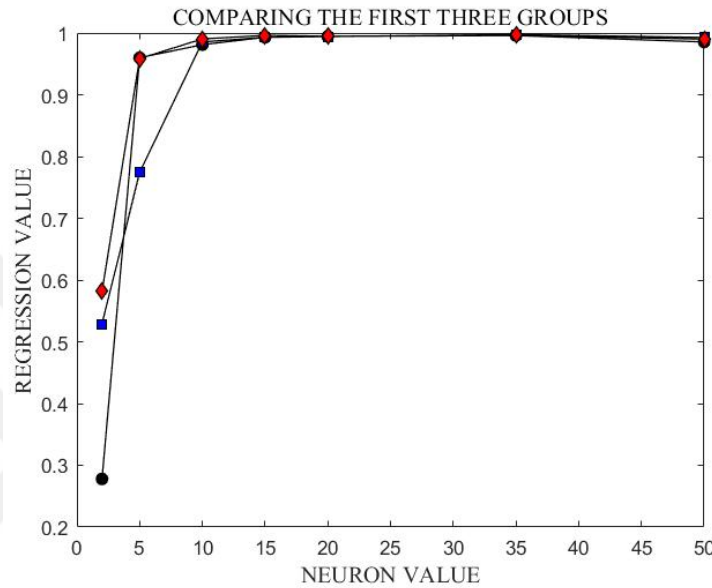


Figure 6.4 : Chart comparing the first three groups.

In the 4th group, the algorithm used was not suitable for the detection of ferroresonance failure, for performing function chosen When the SSE performance function was chosen, a successful training could not be observed. As the number of layers increases, a linear output is expected while a nonlinear process is observed. In 50 layers, the regression value decreased to minus. When regression output between 0 and -1 means the higher level of error for this domain of data train and test are very much larger than the error value for validation. Also this algorithm, it had the chance to observe that the *trainlm* training function does not work efficiently with the SSE performance function and that it works more efficiently with MSE. While *trainlm* training function is expected to work more efficiently with MSE, the result of SSE performance function outputs is that this performance function will not yield rational results. As shown in figure 6.7, it is the graph of the values shown in Table 5.3. As can be seen in this chart, education not offers a predictable chart.

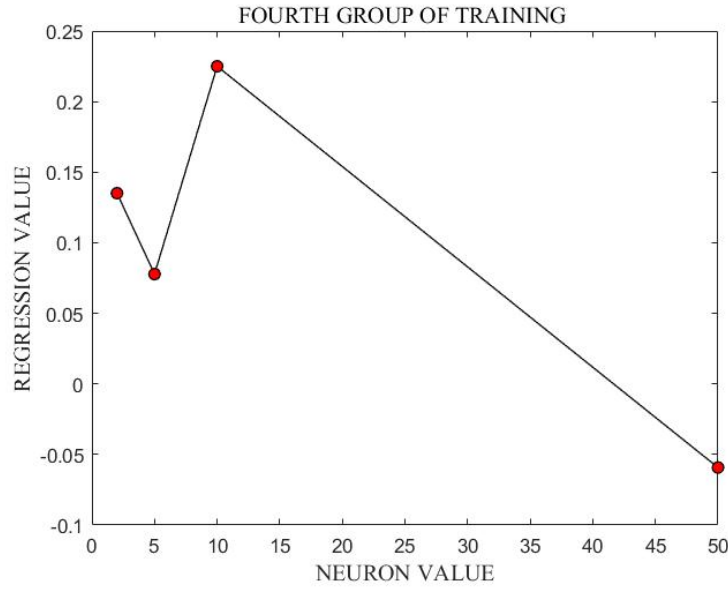


Figure 6.5: Fourth group of training graph.

For fifth group training all, while all inputs in the fifth education remain the same as the values in the first education group, not only the transfer function has been changed from *tansig* to *logsig*. While the training chart of the *logsig* function is expected to be close to the output of the *tansig* function, in figure 6.6 shown that there is a noticeable decline in education in 20th layers, while learning in the 35th layer was close to the first education group, while there was a decrease in 50th layers. The *logsig* function for the training function did not give the expected result in this ferroresonance data, layer numbers and learning dynamics.

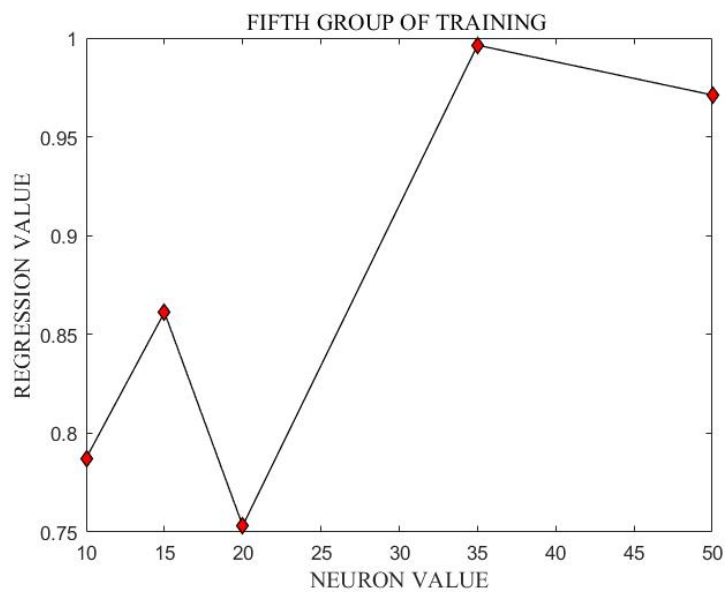


Figure 6.6: Fifth group of training graph.

Figure 6.7 is compared between the first group of training and the fifth group of training it shown that the first group is more successful than the fifth group for nonlinear ferroresonance failure. The *logsig* function did not display a predictable graph, such as the *tansig* function, and this training algorithm failed more than the first group.

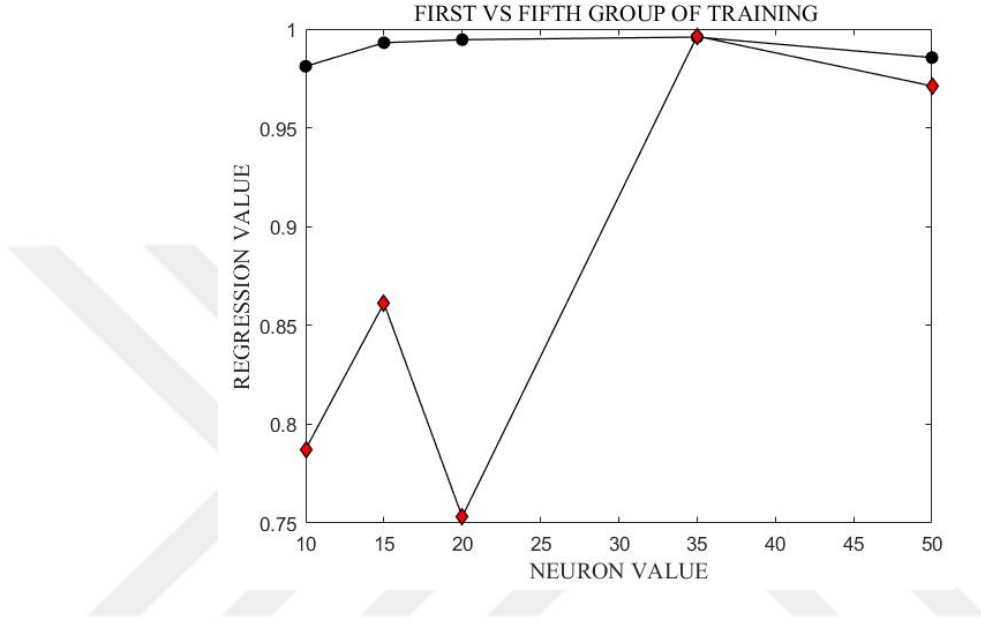


Figure 6.7: Graph comparing the first and fifth learning groups.

For this case for algorithm in backpropagation algorithm, *trainlm* training function, MSE performance function and *tansig* as a transfer function is successful then other algorithm. In nonlinear systems such as ferroresonance, the first third algorithms were successful in neural network application, while the fourth and fifth algorithms could not display a predictable graphic. Although the lack of a specific algorithm is a disadvantage of the neural network, uncertainties about this issue will decrease as successful algorithm trials increase.

This thesis introduces a novel ferroresonance detection technique based on ANNs. This technique has the capability of detect fundamental ferroresonance situations with high degree of accuracy.

In nonlinear systems such as ferroresonance, the first three algorithms were successful in neural network applications, while the fourth and fifth algorithms could not display a predictable graphic.

A regression value of over 99% was detected as from 10th layer to 50th layer in the 3rd group, which is a very successful result. This success started from the 20th layer in the first group. It was observed that the max fail value was effective on learning this is the expected result when looking at the mathematics of the algorithm.

For training algorithm, third training algorithm has best in these groups, but more changes can be made regarding the max fail value and the optimum value can be determined.

ANN techniques, black box sometimes negative because they show they can produce results. So, the forecast tool when used as a traditional method, results found in supporting ANN techniques can be used as an aid. The nature of the problem a properly established network will yield good result. Therefore, suitable network structures should result be investigated according to the problem examined. In this thesis that may best solution for detection of using that ferroresonance signal is feedforward backpropagation algorithm, for training function Levenberg-Marquardt (*trainlm*), for cost function mean square error function, learning function *learnqdm* and transfer function is *tansig*.

Although the lack of a specific algorithm is a disadvantage of the neural network, uncertainties about this issue will decrease as successful algorithm trials increase. Since all error scenarios that may occur in the system are not tried, learning success could not be tried for the error that may occur in another scenario. By using the third training group algorithm, an algorithm can be tried on the failure caused by another scenario.

REFERENCES

- Akinci, T. C., Ekren, N., S, Seker, S., & Yildirim.** (2013). Continuous Wavelet Transform for Ferroresonance Phenomena in Electric Power Systems. *International Journal of Electrical Power & Energy Systems- Elsevier*, 1(44), 403-409.
- Akinci, T. C., Mokryani, G., Gökmen, G., Ekren, N., & Şeker, S.** (2009). Analysis Of Ferroresonance On Single Phase Line Model. 5. *Uluslararası İleri Teknolojiler Sempozyumu (IATS'09)*,.
- Akinci, T.C., & Ekren, N.** (2011). Detection of fenoresonance phenomenon for the west anatolian electric power network in Turkey. *Acta Scientiarum Technology*, 3(33), 273- 279.
- Akinci, T.C., Nogay, H., & Yilmaz.** (2012). Application of Artificial Neural Networks for Defect Detection in Ceramic Materials. *Archives of Acoustics*, 3(37), 279-286.
- Allan, D., & Moore, H.** (2004). Chapter1:Theory and Principles. In *Electric Power Transformer Engineering*. Florida: CRC Press LLC.
- Ang, S. P.** (2010). *Ferroresonance Simulation Studies of Transmission Systems*. The University Of Manchester. Manchester: The University Of Manchester.
- Aydın, M.** (2019). *Derstagram*. Retrieved from <http://www.derstagram.com/manyetik-histerezis-nedir-elektromanyetizma-dersleri/>
- Balaji, S., & K.Baskaran.** (2013). Design And Development Of Artificial Neural Networking (Ann) System Using Sigmoid Activation Function To Predict Annual Rice Production In Tamilnadu. *International Journal of Computer Science, Engineering and Information Technology (IJCSEIT)*, 13-31.
- Basirat, M., & Roth, P. M.** (2019). Learning Task-specific Activation Functions using Genetic Programming. *VISAPP(5)*, 533-540.
- Binev, Y., & Aires-de-Sousa, J.** (2004). Structure-Based Predictions of ¹H NMR Chemical Shifts Using Feed-Forward Neural Networks. *Journal of Chemical Information and Computer Sciences*, 940-945.
- Boduroglu, T.** (1960). *Transformatorlar*. Istanbul: ITU.
- Bose, B. K.** (2001). Artificial neural network applications in power electronics. *IECON'01. 27th Annual Conference of the IEEE Industrial Electronics Society*, 1631-1638. doi:10.1109/IECON.2001.975533
- Boucherot, P.** (1920). Existence de Deux Régimes en Ferro-résonance. *R.G.E.*, 827-828.
- Brink, S., Nease, S., Hasler, P., Ramakrishn, S., Wunderlich, R., Basu, A., & Degnan, B.** (2013). "A Learning-Enabled Neuron Array IC Based Upon Transistor Channel Models of Biological Phenomena. *IEEE Transactions on Biomedical Circuits and Systems*, 71-81. doi:10.1109/TBCAS.2012.2197858
- Chen, X., Caputo, J., & Baghzouz, Y.** (2012). Harmonic analysis of ferroresonance in single-phase transformers. *2012 IEEE 15th International Conference*

- on Harmonics and Quality of Power, 535-540. doi:10.1109/ICHQP.2012.6381277
- Csanyi, E.** (2020). *Electrical Engineering Portal*. Retrieved from <https://electrical-engineering-portal.com/transformer-phenomena>
- Cybenko, G.** (1996). Neural networks in computational science and engineering. *IEEE Computational Science and Engineering*, 1(3), 36-42. doi:10.1109/99.486759
- Çakır, F. S.** (2018). *Yapay Sinir Ağları Matlab Kodları ve MATLAB Toolbox Çözümleri*. Ankara: Nobel.
- Çetin, U.** (2019). Integral Representation of Subharmonic Functions and Differential Equations with Distributional Coefficients. doi:10.13140/RG.2.2.16505.93287
- Dandan, T.** (2003). Güç Sistemlerinde Harmoniklerin Etkisi. *SAU Fen Bilimleri Enstitüsü Dergisi*, 7(1), 129-131.
- Däumling, M. S., & Hofstetter, P. B.** (2018). Simulation of ferroresonance oscillations. In *Ferroresonance Oscillations in Substations with Inductive Voltage Transformers in Medium and High Voltage Systems* (pp. 83-87). Berlin: VDE VERLAG GMBH.
- Däumling, M. S., & Hofstetter, P. B.** (2018). Single-phase ferroresonance oscillation. In *Ferroresonance Oscillations in Substations with Inductive Voltage Transformers in Medium and High Voltage Systems* (pp. 59-61). Berlin: VDE VERLAG GMBH.
- Demuth, H., & Beale, M.** (2004). *Neural Network Toolbox For Use with MATLAB*. The MathWorks.
- Dimitriyev, Y., Haşimov, A., & Nayır, A.** (2003). Elektrik İletim Hatlarında Kaza Açılmalarından Oluşan Gerilimlerin Modelleri. *Elektrik -Elektronik - Bilgisayar Mühendisliği 10. Ulusal Kongresi* (pp. 193-196). Bakü: ELM.
- Du, Y.-C., & Stephanus, A.** (2018). Levenberg-Marquardt Neural Network Algorithm for Degree of Arteriovenous Fistula Stenosis Classification Using a Dual Optical Photoplethysmography Sensor. *Sensors*.
- Endahl, G.** (2017). *Ferroresonance in Power Systems*, Energiforks.
- Ferracci, P.** (1998). *Ferroresonance*. Cahiers Techniques No 190, Groupe Schneider.
- Fyfe, C.** (2005). *Hebbian Learning and Negative Feedback Networks*.
- Gao, X., Gaspar-Cunha, A., Köppen, M., Wang, J., & Schaefer, G.** (2010). *Soft Computing in Industrial Applications: Algorithms, Integration, and Success Stories*. Springer.
- Gavin, H. P.** (2019). The Levenberg-Marquardt algorithm for nonlinear least squares curve-fitting problems. *Duke University*.
- Grassi, M. -F.-Z.** (2007). Face Recognition with Facial Mask Application and Neural Networks., 4507, pp. 709-716. doi:10.1007/978-3-540-73007-1_85
- Gurney, K.** (2003). *An Introduction to Neural Networks*. London: CRC Press.
- Habibi, A. H., & Jahani, H. E.** (2017). *Guide to Convolutional Neural Networks: A Practical Application to Traffic-Sign Detection and Classification*. Switzerland: Springer.
- Hajian, A.** (2018). *Application of Soft Computing and Intelligent Methods in Geophysics*. Springer.
- Hassoun, M., & Clark, D.** (1988). An adaptive attentive learning algorithm for single-layer neural networks. *IEEE 1988 International Conference on Neural Networks, 1*, 431-440. doi:10.1109/ICNN.1988.23876

- Hayash, C.** (1964). *Nonlinear Oscillations in Physical Systems*. New York: McGraw-Hill Book Company.
- Huang, S. H., & H. X.** (2002). Extract intelligible and concise fuzzy rules from neural networks. *Fuzzy Sets and Systems*, 233 – 243.
- Jiles, D. C.** (1993). Frequency Dependence of Hysteresis Curves in "Non-Conducting" Magnetic Materials . *IEEE TRANSACTIONS ON MAGNETICS*, 29(6), 3490-3492.
- Jiles, D., & Atherton, D.** (1983). Ferromagnetic hysteresis. *IEEE Transactions on Magnetics*(19), 2183-2185.
- Karlik, B., & Olgac, A. V.** (2011). Performance Analysis of Various Activation Functions in Generalized MLP Architectures of Neural Networks. *International Journal of Artificial Intelligence And Expert Systems (IJAE)*, 111-122.
- Komendantskaya, E.** (2011). Unification neural networks: unification by error-correction learning,. *Logic Journal of the IGPL*, 821-847.
- Lin, C. E., Wei, J., Huang, C. -, & Huang, C.** (1989). A new method for representation of hysteresis loops. *IEEE Transactions on Power Delivery*, 413-420. doi:10.1109/61.19231.
- Lin, J.-W.** (2017). Artificial Neural Network Related to Biological Neuron Network: A Review. *Advanced Studies in Medical Sciences*(5), 55-62.
- Lippmann, R.** (1987). An introduction to computing with neural nets. *EEE ASSP Magazine*, 4-22. doi:10.1109/MASSP.1987.1165576
- Martinez, R. D., Fontenla, R., Oscar, A., & Alonso, B.** (2012). Nonlinear single layer neural network training algorithm for incremental,nonstationary and distributed learning scenarios. *Pattern Recognition*, 4536-4546.
- Mehrotra, K., Mohan, C. K., & Ranka, S.** (2000). *Elements of Artificial Neural Networks*. Massachusetts: MIT Press.
- Mijwil, M. M.**, (2018). *Artificial Neural Networks Advantages and Disadvantages*. [Online] Available at: <https://www.linkedin.com/pulse/artificial-neural-networks-advantages-disadvantages-maad-m-mijwel/>[Accessed 02 06 2020].
- Mishra, M., & Srivastava, M.** (2014). A View of Artificial Neural Network. *IEEE International Conference on Advances in Engineering & Technology Research*.
- Mork, B. A.** (2006). Understanding and Dealing with Ferroresonance. *Minnesota Power Systems Conference* .
- Moses, P. S., & Masoum, M. A.** (2009). Modeling ferroresonance in asymmetric three-phase power transformers. *Australasian Universities Power Engineering Conference*, 1-6.
- Nguyen, D., & Widrow, B.** (1990). Improving the learning speed of 2-layer neural networks by choosing initial values of the adaptive weights. *CNN International Joint Conference on Neural Networks*, 3, 21-26. doi:1109/IJCNN.1990.137819
- Omer, A., Akinci ,T.C, Erdemir, G., & Seker, S.** (2019). Analysis of Instantaneous Frequency, Instantaneous Amplitude and Phase Angle of Ferroresonance in Electrical Power Networks. *Journal of Electrical Engineering*, 6(70), 1-5.
- Pan, H. & Chen, B.,**(2012) Intelligent Fault Diagnosis Based on ANN: A Review. Paris, *The 2nd International Conference on Computer Application and System Modeling*.

- Park, D. C., El-Sharkawi, M. A., Marks, R. J., Atlas, L. E., & Damborg, M. J.** (1991). Electric load forecasting using an artificial neural network. *IEEE Transactions on Power Systems*, 6, 442 - 449.
- Patel, D., & Stonham, T. J.** (1991). A single layer neural network for texture discrimination. *IEEE International Symposium on Circuits and Systems*, 5, 2656-2660. doi:10.1109/ISCAS.1991.176092
- Patsios, C., Tsampouris, E., Beniakar, M., Rovolis, P., & Kladas, A. G.** (2011). Dynamic Finite Element Hysteresis Model for Iron Loss Calculation in. *IEEE TRANSACTIONS ON MAGNETICS*, 47(5), 1130-1133.
- Pejic, M., Tokic A., Kasumovic, M., & Akinci T.C.** (2017). Laboratory Ferroresonance Measurements in Power Transformers. *Elektrotehniski Vesnik*, 4(84), 195-199.
- Priddy, K. L., & Keller, P. E.** (2005). *Artificial Neural Networks an Introduction*. Washington: SPIE PRESS.
- Reed, R., & MarksII, R. J.** (1999). *Neural Smithing: Supervised Learning in Feedforward Artificial Neural Networks*. London: MIT Press.
- Rojas, R.** (1996). *Neural Networks*. Berlin: Springer-Verlag.
- Rosa, F. C.** (2006). *Harmonics and Power System*. New York: CRC Press.
- Rudenberg, R.** (1950). *Transient Performance of Electric Power Systems*. New York, NY: McGraw-Hill Book Company.
- S.V.Kulkarni, & S.A.Khaparde.** (2004). *Transformer Engineering Design and Practice*. New York: M ARCEL DEKKER, INC.
- Sazlı, M.** (2006). A Brief Review of Feed forward Neural Networks. *Commun. Fac. Sci. Univ. Ank. Series*, 11-17.
- Seker, S., Akinci, T. C., & Taskin, S.** (2011). Spectral and statistical analysis for ferroresonance phenomenon in electric power systems. Springer-Verlag.
- Sergio, G., Marsette, V., & Dimitrios, K.** (2015). A three-toe biped foot with Hall-effect sensing. *2015 IEEE/RSJ International Conference on Intelligent Robots and Systems (IROS)*, (pp. 360-365).
- Serhat, S., Akinci, T.C., & Taskin, S.** (2012). Spectral and Statistical Analysis for Fenoresonance Phenomenon in Electric Power System. *Electrical Engineering*, 2(94), 117-124.
- Sharbain, H. A., Osman, A., & El-Hag, A.** (2017). Detection and identification of ferroresonance. *2017 7th International Conference on Modeling, Simulation, and Applied Optimization (ICMSAO)*, (pp. 1-4). Sharjah.
- Siddique, N., & Adeli, H.** (2013). *Computational Intelligence: Synergies of Fuzzy Logic, Neural Networks and Evolutionary Computing* (1 ed.). West Sussex: Wiley.
- Singh, S., Singh, D. S., & Kumar, S.** (2013). Modified Mean Square Error Algorithm with Reduced Cost of Training and Simulation Time for Character Recognition in Backpropagation Neural Network. (pp. 137-145). Odisa: Springer International Publishing Switzerland.
- Specht, D. F.** (1991). A General Regression Neural Network. *IEEE Transactions On Neural Networks*, 2(6), 568-576.
- Sutton, R. S., & Barto, A. G.** (1998). *Introduction to Reinforcement Learning*. Cambridge: MIT Press.
- Udpa, S., & Lord, W.** (1985). A Fourier descriptor model of hysteresis loop phenomena. *IEEE Transactions on Magnetics*, 21, 2370-2373. doi:10.1109/TMAG.1985.1064156.

- Valverde, V. a.** (2012). Ferroresonance in Voltage Transformers: Analysis and Simulations. *Przegląd Elektrotechniczny*(88).
- Valverde, V., Mazón, J., Buigues, G., & Zamora, I.** (2012). Ferroresonance Suppression in Voltage Transformers. *Przegląd Elektrotechniczny*, 137-140.
- Wahyudi, M., Negara, M. Y., Asfani, D. A., Satriyadi, G. N., Hernanda, & Fahmi, D.** (2017). Application of Wavelet Cumulative Energy and Artificial Neural Network for Classification of Ferroresonance Signal During Symmetrical and Unsymmetrical Switching of Three-Phases Distribution Transformer. *2017 International Conference on High Voltage Engineering and Power System* (pp. 394-399). Bali: IEEE.
- Wang, Y., Li, Y., Song, Y., & Rong, X.** (2020). The Influence of the Activation Function in a Convolution Neural Network Model of Facial Expression Recognition. *Applied Sciences*.
- Watson, C., Kirkcaldie, M., & Paxinos, G.** (2010). *The Brain: An Introduction to Functional Neuroanatomy*. London: ELSEVIER.
- Zhang, J., & Morri, A. J.** (1998). A Sequential Learning Approach for Single Hidden Layer Neural Networks. *Neural Networks*, 65-80.
- Zhang, Y., Malik, O. P., & Chen, G. P.** (1995). Artificial neural network power system stabilizers in multi-machine power system environment. *IEEE Transactions on Energy Conversion*, 147-155.



APPENDICES

APPENDIX A:

NN7, NN23, NN8, NN31 from the first training group output's performance and regression outputs are below. For first training group, chosen network type is as feed-forward back-propagation, for training function preferred *trainlm*, *learnngdm* is chosen as adaptation learning function, for performance function MSE and transfer function TANSIG, for epochs 1000 and max fail 1000

NN7

For NN7 neuron number is 2. We can see figure A.1 performance of NN7. Regression output is not on below there by, as regression output is below 0.95. In the chart, the network training has ended at the 36st iteration but it has acquired the best performance on the 18th iteration.

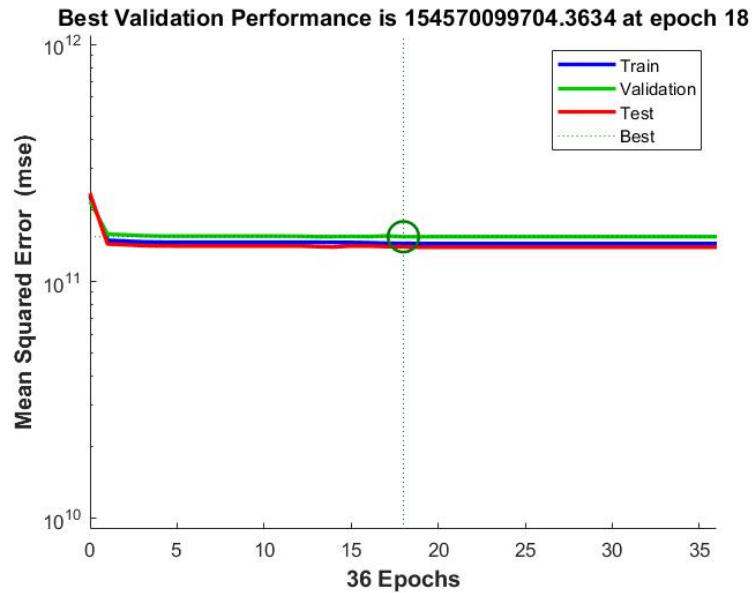


Figure A.1: Performance plot for NN7.

NN23

For NN23 neuron number is 5. The figure 5.3 shown that performance output of NN23 and figure A.2 shown that regression output of NN23 training. In the chart, the network training has ended at the 1000th iteration but it has acquired the best performance on the 37th. The regression output for 5 neuron input and target data match 0,96.

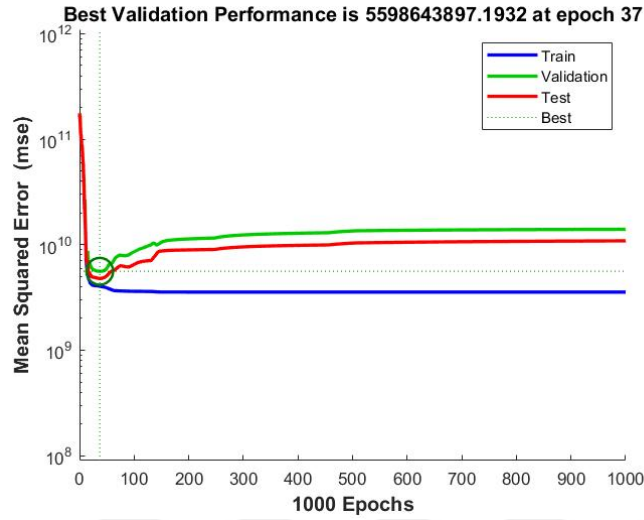


Figure A.2 : Performance plot for NN23.

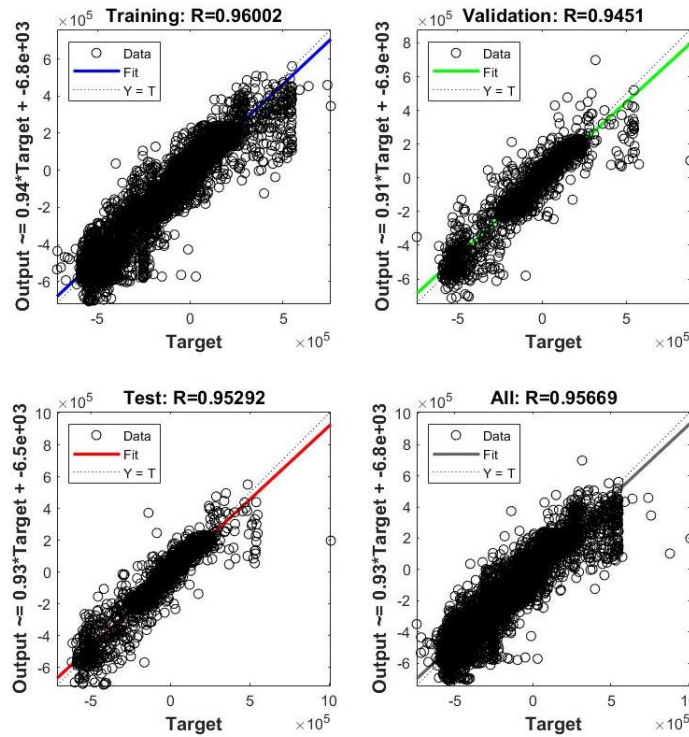


Figure A.3 : Regression plot for NN23.

NN8

For NN8 neuron number is 10. The figure A.4 shown that performance output of NN8 and figure A.5 shown that regression output of NN8 training. In the chart, the network training has ended at the 1000th iteration but it has acquired the best performance on the 28th. The regression output for 10 neuron input and target data match 0,98113

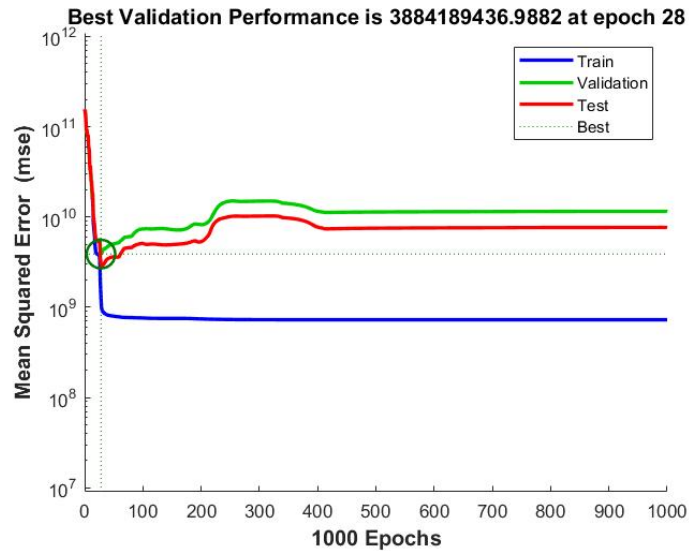


Figure A.4 : Performance plot for NN8.

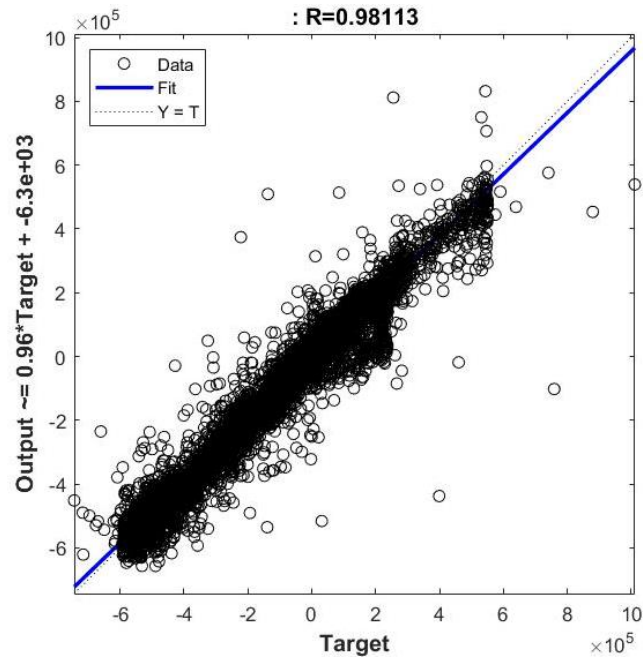


Figure A.5 : Regression plot for NN8.

NN31

For NN31, neuron number is 15. Figure A.6 shown that performance output of NN31 in the chart, the network training has ended at the 1000th iteration but it has acquired the best performance on the 9th. The regression output of 15 neuron of first training group input and target data match 0,99306 and figure A.7 shown that regression output of NN31 training.

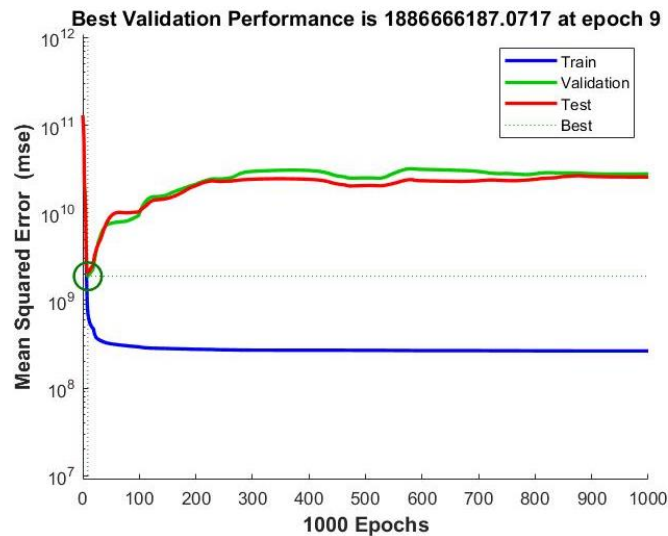


Figure A.6 : Performance plot for NN31.

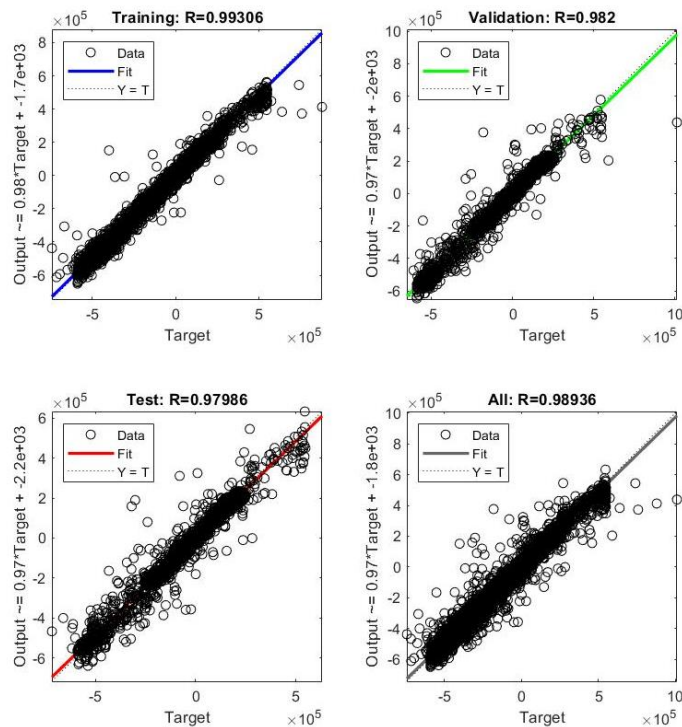


Figure A.7 : Regression plot for NN31.

NN4, NN22, NN5, NN17 from the second training group output's performance and regression outputs are below. For second training group, chosen network type is as feed-forward back-propagation, chosen network type is as feed-forward back-propagation, for training function preferred *trainlm*, *learnngdm* is chosen as adaptation learning function, for performance function MSE and transfer function TANSIG, for epochs 1000 and max fail 500

NN4

For NN4 neuron number is 2. The figure A.8 shown that performance output of NN4.

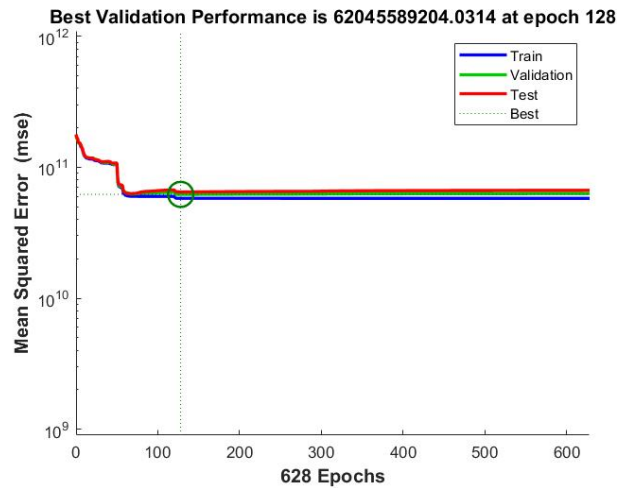


Figure A.8 : Performance plot for NN4.

NN22

For NN22 neuron number is 5. Figure A.9 shown that performance output of NN22 and figure A.10 shown that regression output of NN22 training.

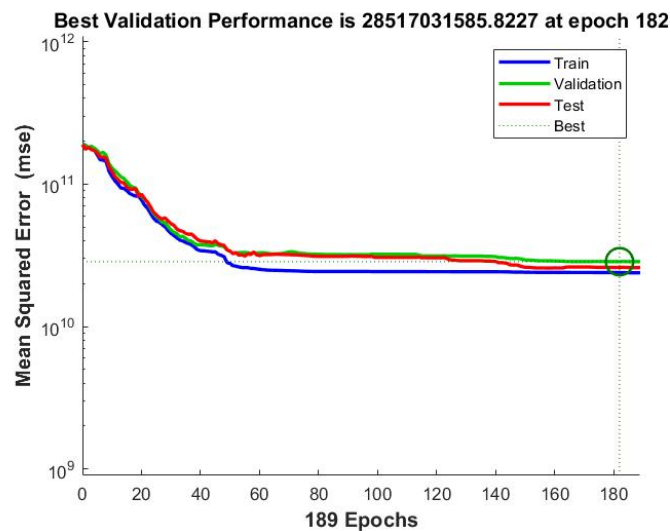


Figure A.9 : Performance plot for NN22.

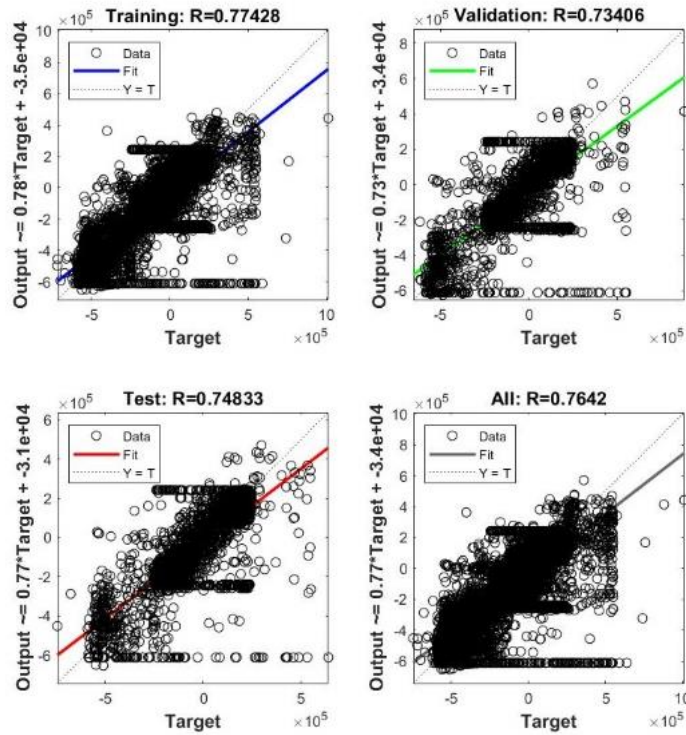


Figure A.10 : Regression plot for NN22.

NN5

For NN5 neuron number is 10. We can see figures performance of NN5. Figure A.11 shown that performance output of NN5 and figure A.12 shown that regression output of NN5 training.

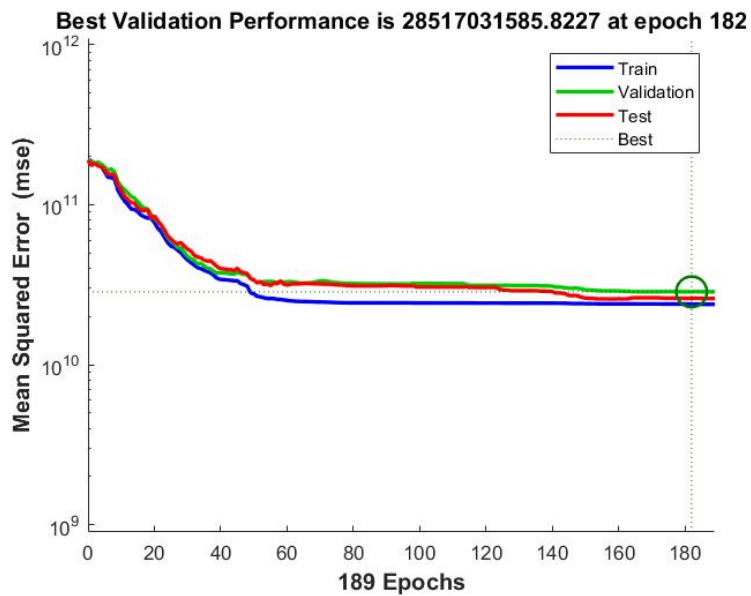


Figure A.11 : Performance plot for NN5.

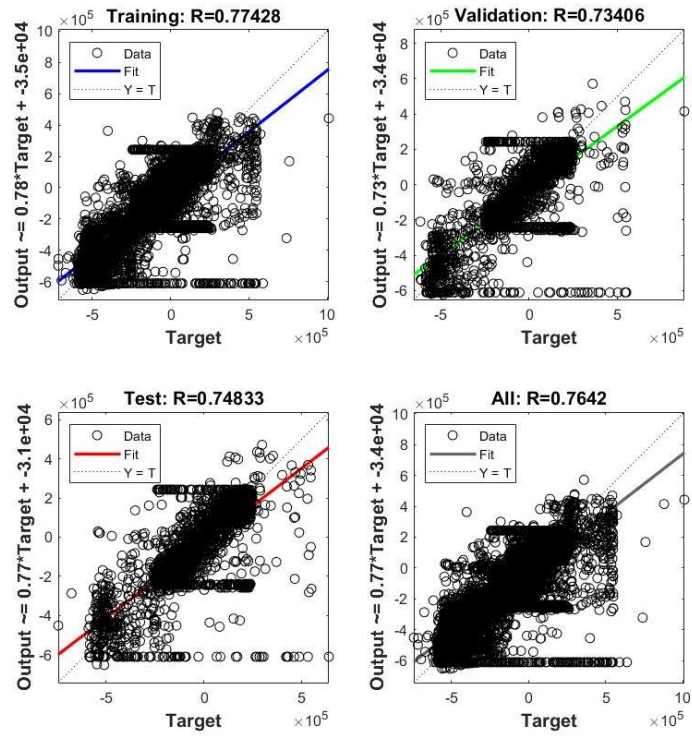


Figure A.12 : Regression plot for NN5.

NN17

For NN17 neuron number is 15. Figure A.13 shown that performance output of NN17 and figure A.14 shown that regression output of NN17 training.

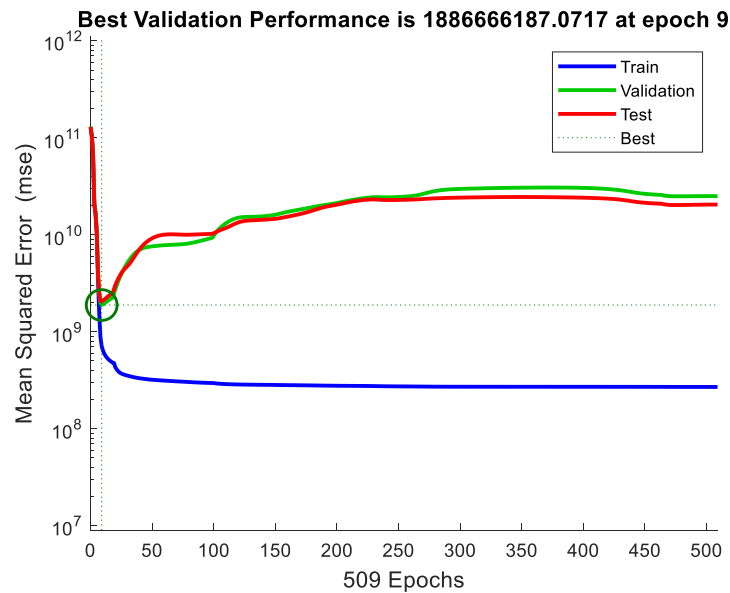


Figure A.13 : Performance plot for NN17.

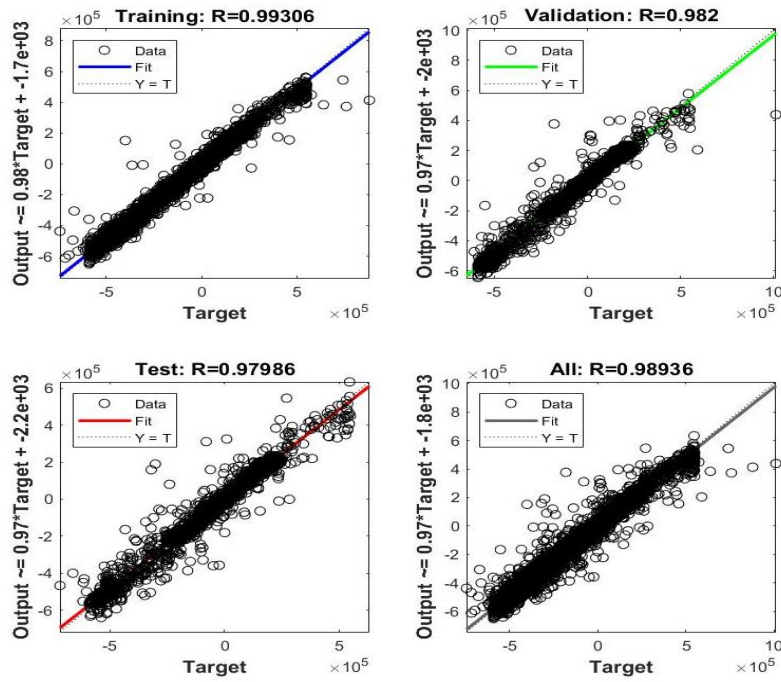


Figure A.14: Regression plot for NN17.

NN20, NN21, NN25, NN26, NN27 from the third training group output's performance and regression outputs are below.

NN20

For NN20 is neuron number 2. We can see figure A.15 performance of NN20.

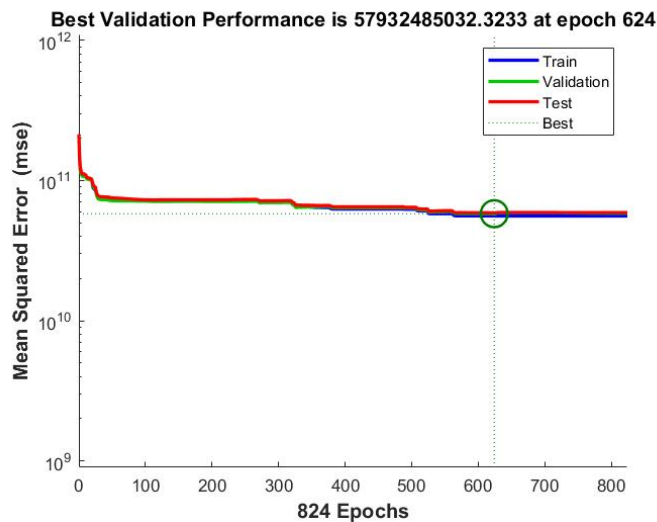


Figure A.15: Performance plot for NN20.

NN21

For NN21 neuron number is 5. The figure A.16 shown that performance output of NN21 and figure A.17 shown that regression output of NN21 training.

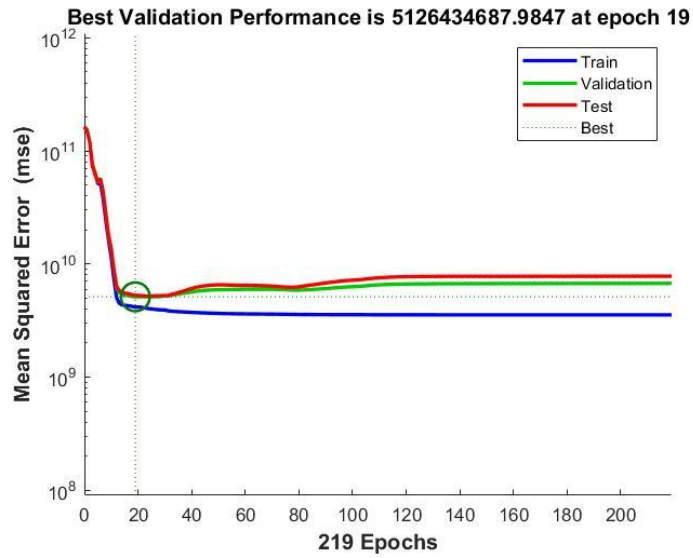


Figure A.16 : Performance plot for NN21.

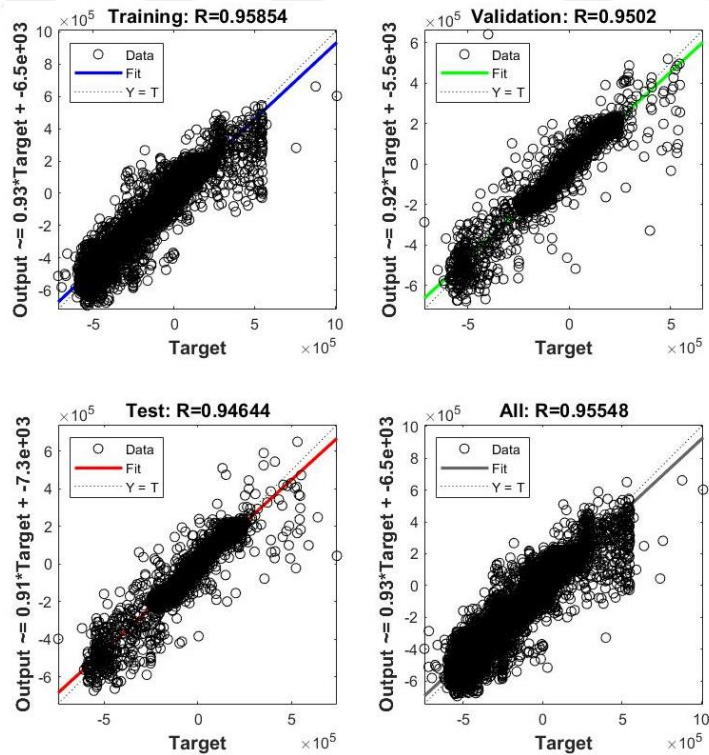


Figure A.17 : Regression plot for NN21.

NN25

For NN25 neuron number is 10. The figure A.18 shown that performance output of NN33 and figure A.19 shown that regression output of NN25 training.

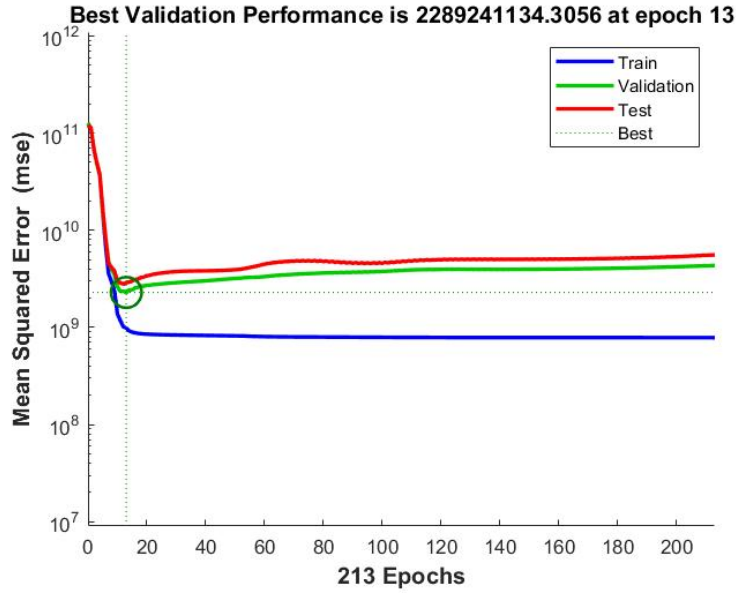


Figure A.18 : Performance plot for NN25.

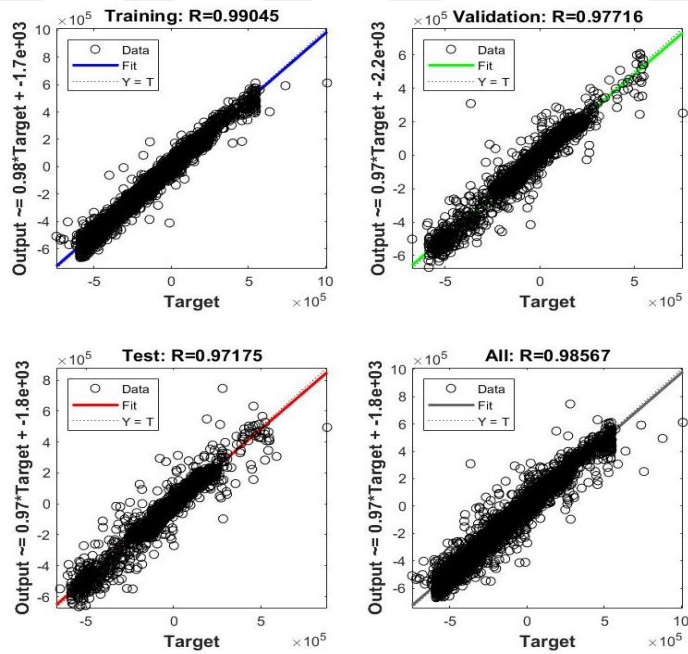


Figure A.19 : Regression plot for NN25.

NN26

For NN26 neuron number is 15. The figure A.20 shown that performance output of NN26 and figure A.21 shown that regression output of NN26 training.

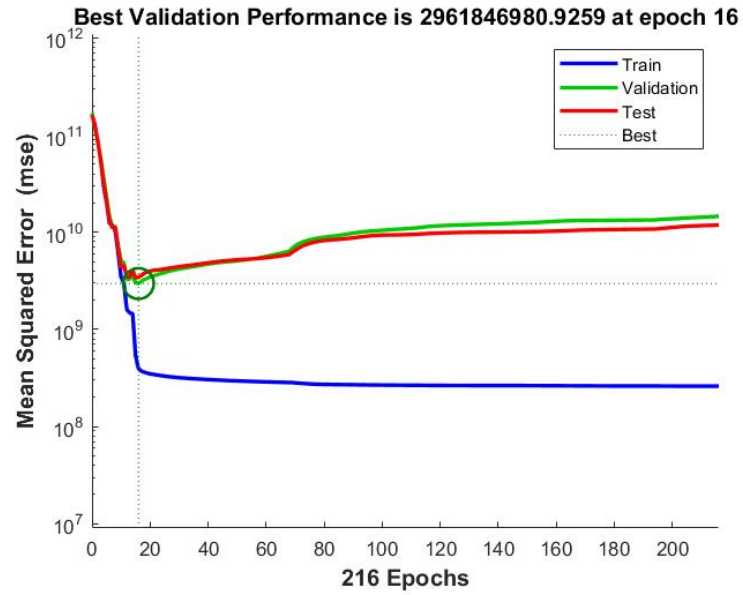


Figure A.20: Performance plot for NN26.

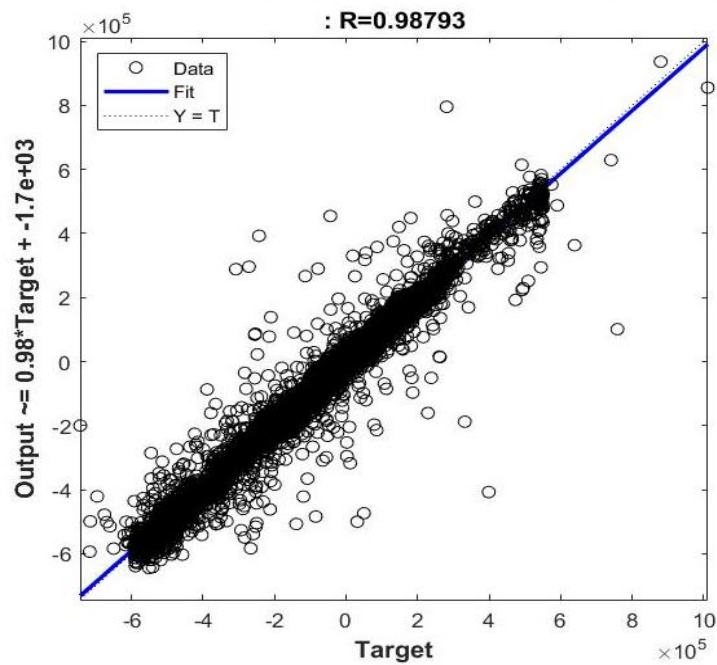


Figure A.21: Regression plot for NN26.

NN27

For NN27 neuron number is 20. The figure A.22 shown that performance output of NN27 and figure A.23 shown that regression output of NN27 training.

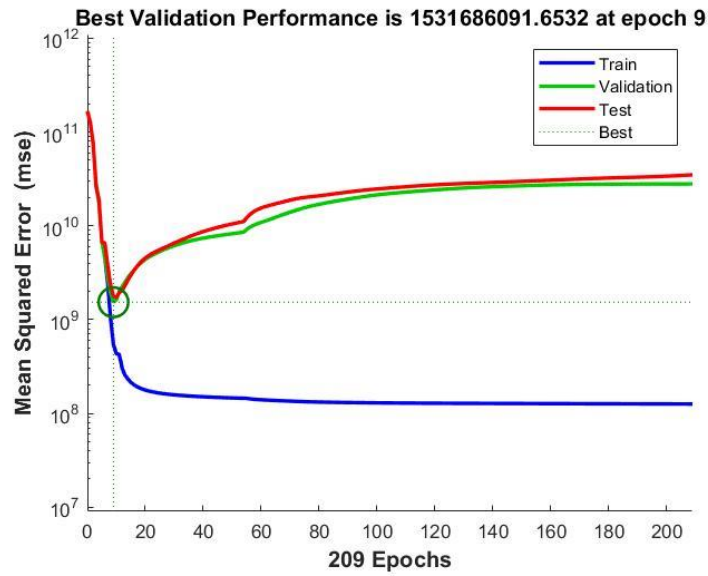


Figure A.22 : Performance plot for NN27.

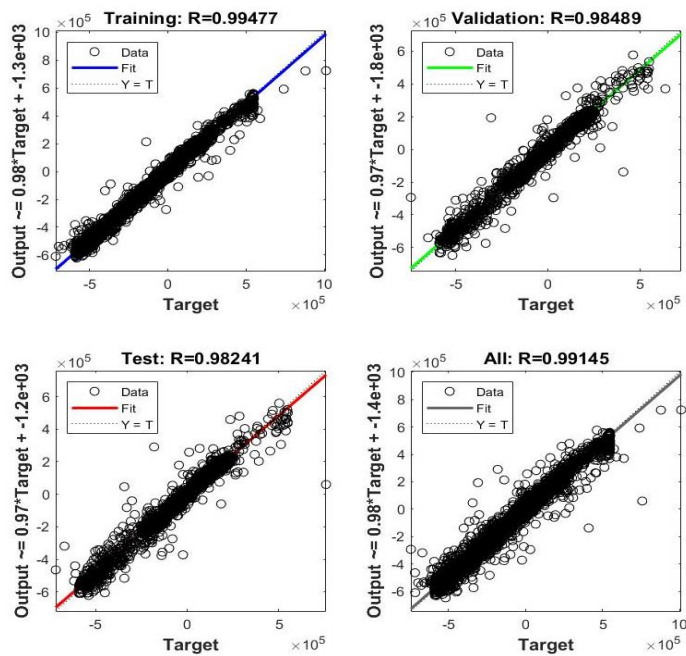


Figure A.23 : Regression plot for NN27.

CURRICULUM VITAE



Name Surname : Gizem Kulaklı
Place and Date of Birth : Ankara/31.03.1991
E-Mail : gkulakliitu@gmail.com

EDUCATION :

- **M.Sc** : 2020, Technische Universität Dresden, Institute Of Electrical Power Systems And High Voltage Engineering, Erasmus M.Sc. Thesis Program
- **M.Sc** : 2020, Istanbul Technical University, Department of Electrical Engineering, Electrical Engineering Master's Program
- **B.Sc.** : 2014, Gazi University, Electrical-Electronics Engineering
- **B.Sc.** : 2020, Anadolu University, Business Management

PROFESSIONAL EXPERIENCE AND REWARDS:

- 2012- FUJITSU (Intern Engineer)
- 2013-ENERJISA (Intern Engineer)
- 2014-2014 EATON (Re&De Engineer)
- 2014-2016 EATON (Oil Type and Dry Resign Type Production-Process, Maintenance Engineer)
- 2016-2017 EATON (Oil Type and Dry Resign Type Distribution Transformer Design Engineer)
- 2017-2018 BEST TRANSFORMER (Senior Design Engineer)
- 2018-2019 ITU (Student Assistant at Cognitive Laboratory)
- 2019-2019 SCHNEIDER ELECTRIC (Design Engineer)

PUBLICATIONS, PRESENTATIONS AND PATENTS ON THE THESIS:

- **Kulaklı G**, Akinci T.C .2018. PSD and Wavelet Analysis Of Signal From Healthy And Epileptic Patient, *Journal of Cognitive Systems Vol 3, No.1, pp 15-17*.
- **Kulaklı G**, İlaslan M.F., Akgün O, Akinci T.C. 2019. Çok Çözünürlüklü Dalgacık Analizi İle İstanbul Rüzgar Hızı Analizi, Mühendislikte Yeni Yaklaşımlar, (Editor: Mine Nazan Kerimak Öner; Recep Onur Uzun), Berikan Matbaacılık, (ISBN: 978-605-7634-10-8), **2019**. pp.255-266.
- Akgün, Ö. Varol, H.S., İlaslan, M.F., **Kulaklı, G.**, Akinci, T.C., *Determination of Hearth Valve Stenosis and Failure Using Zero-Poles Map*, 4th International Scientific Research Congress (UBAK), 14-17 Feb., **2019**, Yalova, Turkey, pp.215-223.

BAP Uygulama Yönergesinin ilgili maddesi uyarınca; BAP Koordinasyon Birimi tarafından desteklenen projeler kapsamında tamamlanan tezlerde “Bu çalışma; İTÜ Bilimsel Araştırma Projeleri Birimince desteklenmiştir. Proje numarası: 41846 (The Research Fund of Istanbul Technical University supported this work. Project Number: 41846)”

